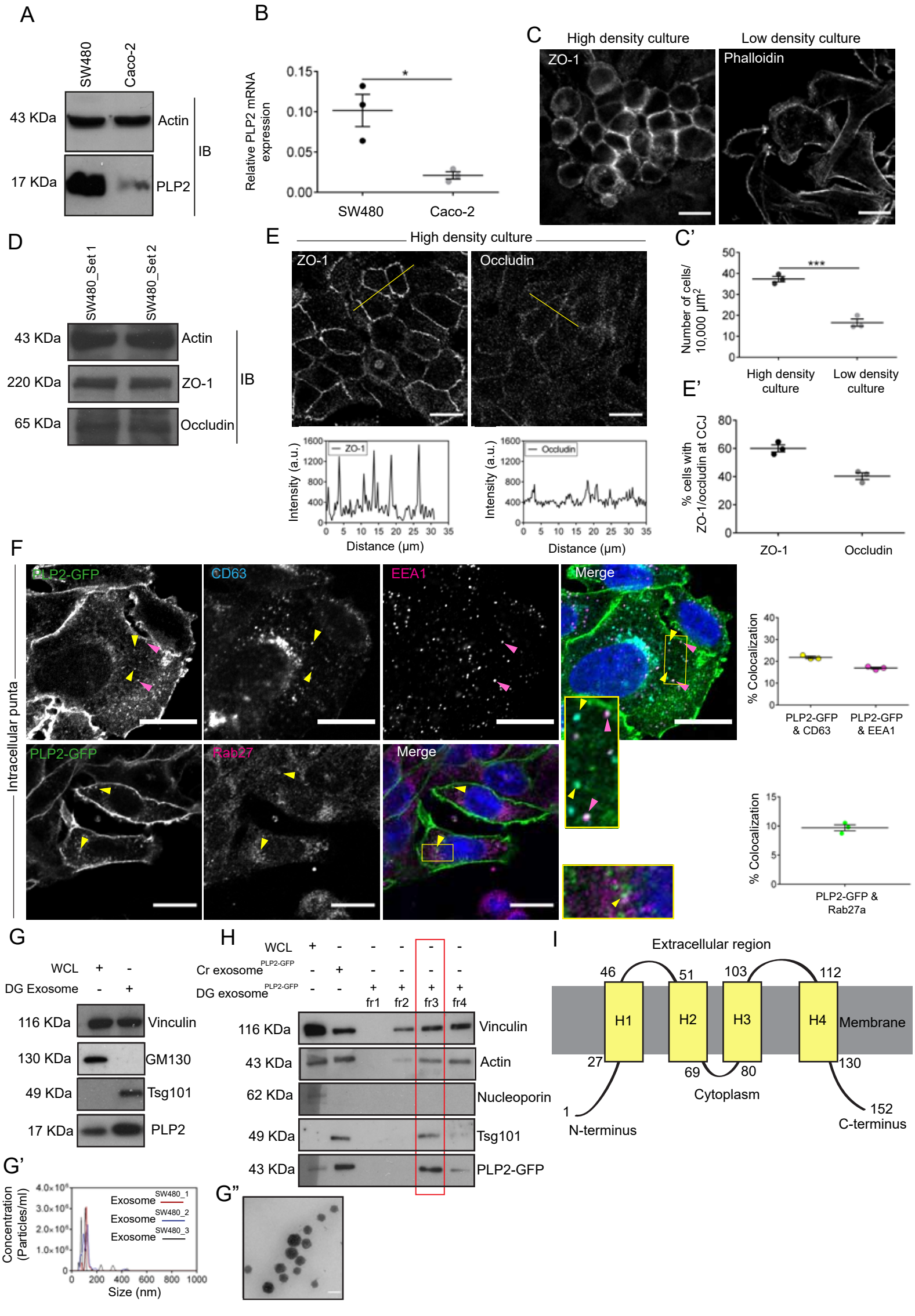
A
SW480
Caco-2
43 KDa
Actin
IB
17 KDa
PLP2
B
Relative PLP2 mRNA expression
0.15
0.10
0.05
0.00
*
SW480
Caco-2
C
High density culture
Low density culture
ZO-1
Phalloidin
D
SW480_Set 1
SW480_Set 2
43 KDa
Actin
220 KDa
ZO-1
65 KDa
Occludin
IB
E
High density culture
ZO-1
Occludin
Intensity (a.u.)
Distance (μm)
C'
Number of cells/ 10,000 μm2
***
High density culture
Low density culture
E'
% cells with ZO-1/occludin at CCJ
ZO-1
Occludin
F
Intracellular punta
PLP2-GFP
CD63
EEA1
Merge
Rab27
% Colocalization
PLP2-GFP & CD63
PLP2-GFP & EEA1
PLP2-GFP & Rab27a
G
WCL
DG Exosome
116 KDa
Vinculin
130 KDa
GM130
49 KDa
Tsg101
17 KDa
PLP2
G'
Concentration (Particles/ml)
Exosome SW480_1
Exosome SW480_2
Exosome SW480_3
Size (nm)
G"
H
WCL
Cr exosome PLP2-GFP
DG exosome PLP2-GFP
fr1
fr2
fr3
fr4
116 KDa
Vinculin
43 KDa
Actin
62 KDa
Nucleoporin
49 KDa
Tsg101
43 KDa
PLP2-GFP
I
Extracellular region
46
51
103
112
H1
H2
H3
H4
Membrane
27
69
80
130
1
Cytoplasm
152
N-terminus
C-terminus

Fig. S1. PLP2 is preferentially expressed in the migratory colonic epithelial cell line and secreted via exosomes. A) Total protein extracts (30 µg/well) from the indicated cells were immunoblotted to detect the cellular protein level of PLP2. B) The expression level of PLP2 in the indicated cell lines, normalized to the expression level of GAPDH. Data represented as scatter plots showing means±SEM (N=3). C) SW480 cells show free edge actin-rich extensions in low-density culture. In high-density culture, lateral cell-cell junctions with the distinct presence of tight junction protein ZO-1 were observed. C') On average, 37 cells and 17 cells per 10,000 μm^2 were taken as a measure for high (n=3184) and low-density (n=1433) culture, respectively—data represented as means ±SEM (N=3). D) ZO-1 and occludin protein levels are detected by immunoblotting of the total protein extracts (30 µg/well) from SW480 cells. E) High density culture of SW480 cells show distinct localization of ZO-1 in the cell-cell junctions compared to the intracellular pool, whereas occludin localization to the cell-cell junction versus cytosolic pool is less distinct. The intensity plots represent fluorescence intensity (y-axis) against distance (x-axis). E') Densely grown SW480 cells form lateral cell-cell junctions, of which 60.56% of cells contain ZO-1, and 44.71% contain occludin in two or more lateral junctions of a cell. Total number of cells quantified n=1807 (ZO-1) and n=1542 cells (occludin) (N=3). F) Part of vesicular PLP2-GFP colocalized with CD63 (object-based colocalization value 21.83±0.02% measured over 1268 cells, N=3), with EEA1 (object-based colocalization value 16.94±0.019% measured over 1268 cells, N=3) and with Rab27a (object-based colocalization value 9.6 ±0.012% measured over 458 cells, N=3); colocalized puncta indicated by yellow arrowheads for PLP2-GFP:CD63 and PLP2- GFP:Rab27; by pink arrowheads for PLP2-GFP:EEA1; refer to method section 'confocal image analysis' for details on object-based colocalization. G) Endogenous PLP2 is secreted and enriched in exosomes purified from SW480 cells. SW480 whole cell lysate (WCL) and density gradient purified exosomes (DG Exosome) were lysed to extract total proteins and immunoblotted with PLP2 antibody along with positive (Tsg101) and negative (GM130) markers for exosomal proteins. Vinculin was used as a loading control. G') Size distribution of exosomes purified from SW480 cells ($exosome^{SW480}$) measured by nanoparticle tracking analysis or NTA (N=3). G") Characterization of $exosome^{SW480}$ by transmission electron microscopy (TEM). H) SW480 cells stably overexpressing PLP2-GFP were subjected to exosome purification, a crude (Cr $exosome^{PLP2\text{-}GFP}$), and density gradient purified exosomes (DG $exosome^{PLP2\text{-}GFP}$) were lysed and immunoblotted for the presence of PLP2-GFP in the exosome fractions along with positive exosome marker Tsg101. I) Predicted tetra-helical trans-membrane topology of the 152 amino acid long PLP2 with both N and C-terminal end in the cytoplasm. The cartoon is drawn as per the PSIPRED secondary structure prediction. All panels: n=number of cells, N= number of experiments; Statistical significance was calculated using a paired two-tailed t-test (B) and an unpaired two-tailed t-test (C'); *, $P<0.05$; ***, $P < 0.0005$; Scale bars= 15 µm (C, E and F) and 100 nm (G").

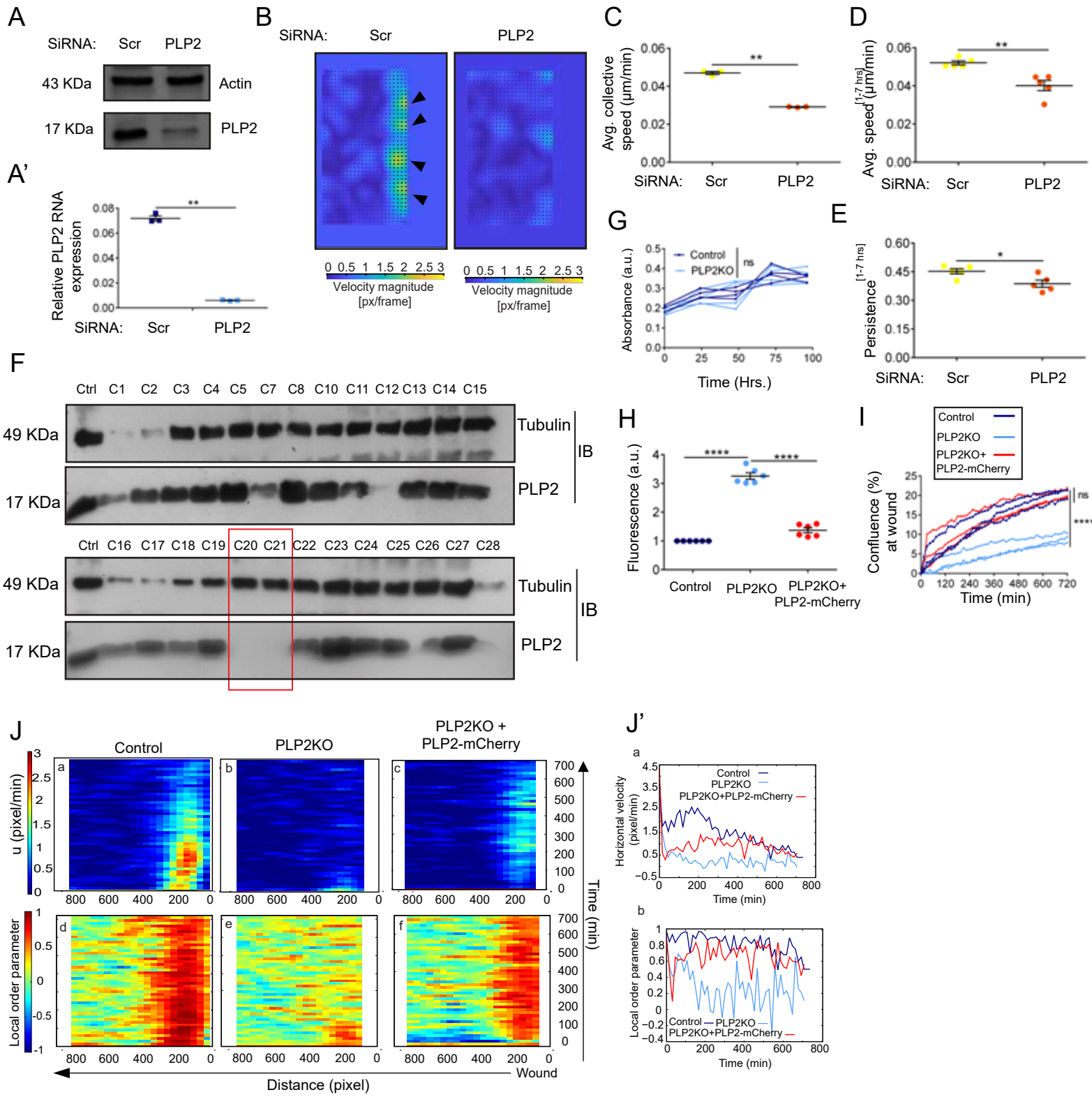

Fig. S2. PLP2 plays a crucial role in collective cell migration. A) and A') SW480 cells were transfected with SMARTpool SiRNA against PLP2 and cells were harvested and lysed 72 hrs post-transfection to isolate protein and RNA in respective cases. Knock-down efficiency was validated at A) protein level (actin as a loading control) by western blot and A') mRNA level (relative to GAPDH) by q-RTPCR. Cells transfected with non-targeting SiRNA SMARTpool (Scr control) were used as negative controls. B) to E) Wound scratch assay performed on cells transfected with non-targeting (Scr) or PLP2 targeting (PLP2) SiRNA SMARTpools. B) and C) PIV analysis. B) Velocity heatmaps (1 pixel = 0.586 μm; 1 frame= 15 mins; high-speed zones: yellow regions pointed with black arrows) and C) Average collective speed measured between 1 to 7 hrs post-wound. Data represented as scatter plots showing mean±SEM from three independent experiments. D) and E) Track Analysis. Individual cells tracked from the first four layers of the progressing cell sheet. D) Average speed and E) Persistence measured between 1 to 7 hrs post-wound. D) and E) Data represented as scatter plots with mean±SEM from five independent experiments (N=5); n= 383 (80+73+83+81+66) for Scr control and n= 347 (70+57+59+81+80) for PLP2 depleted cells. F) Different clones of SW480-PLP2KO were obtained after cells were transfected with Cas9 protein complexed with either control sgRNA (Control cells) or sgRNA-targeting PLP2 (PLP2KO cells). The knockout efficiency was determined by immunoblotting for PLP2 and tubulin (loading control). C1 to C28 represent different clones during PLP2KO screening. Red box indicates selected clones. C20 was used for further experiments. G) MTT assay performed on control and PLP2KO cells at 0, 24, 48, 72, and 96 hrs post-seeding of 20,000 cells. Data represented as four independent experiments. H) The paracellular flux of 70 KDa FITC-dextran through monolayers formed by control, PLP2KO, and PLP2KO cells overexpressing PLP2-mCherry. The amount of FITC-dextran diffused to the basolateral side of the monolayer was normalized by the average value obtained from control cells. Values given represented as scattered plots showing mean±SEM from six independent experiments. I) The confluence of cells within the wound area during wound closure. Data represented individually as three independent experiments. J) Kymographs showing spatiotemporal dynamics of horizontal velocity (u) (pixel/min) (a,b,c) and local order parameter (d,e,f). The distance at the wound edge was taken as zero with gradual increment towards (-) x-direction (refer to Fig 2B). J') Time dependence of u (pixel/min) (a) and local order parameter (b) at a given X averaged over Y in respective cells. X= 147 for control, 220 for PLP2KO, 159 for PLP2KO+PLP2-mCherry. All panels: N= number of experiments; n= number of cells/ tracks. Statistical significance was calculated using a paired two-tailed t-test (For A' and G), an unpaired two-tailed t-test (For C, D and E) and one way ANOVA (For H and I). ns=non-significant; *, $P<0.05$; **, $P<0.005$; ****, $P<0.0001$.

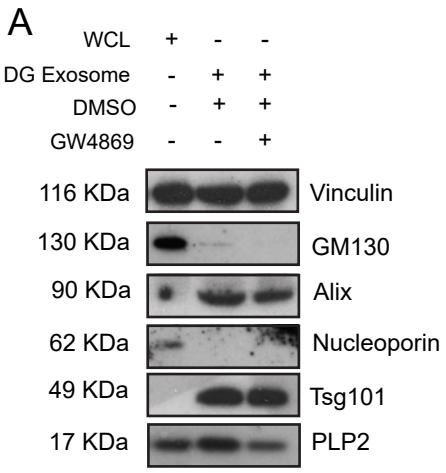

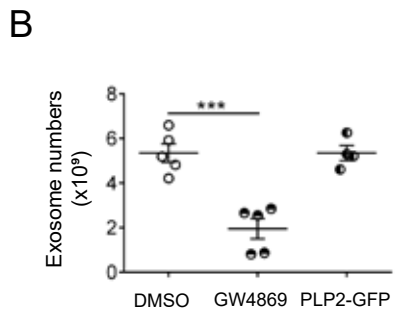

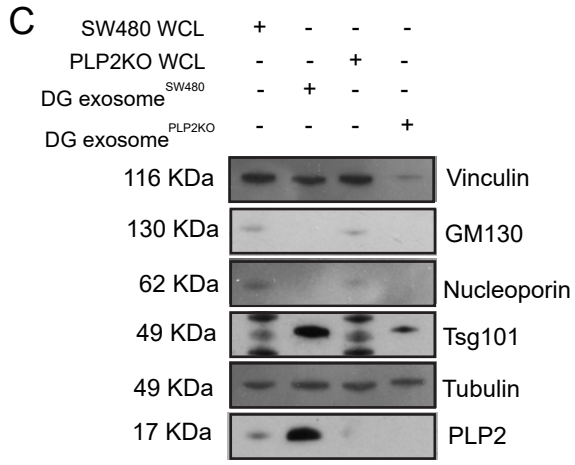

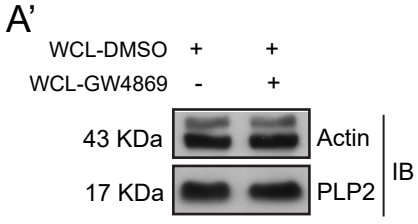

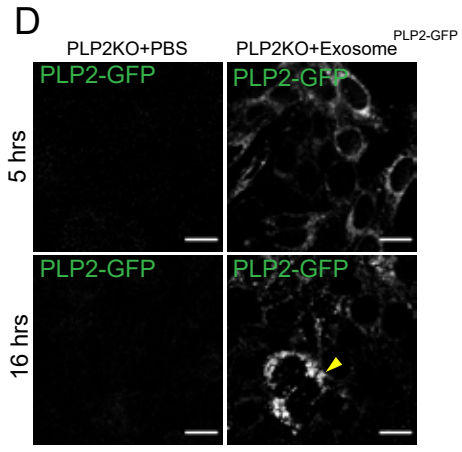

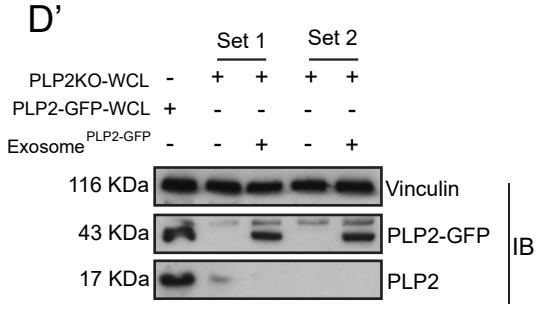

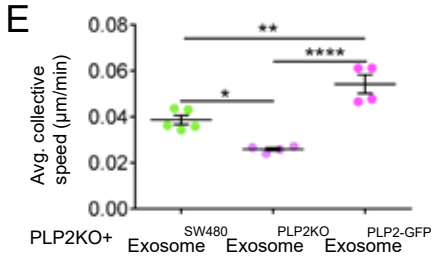

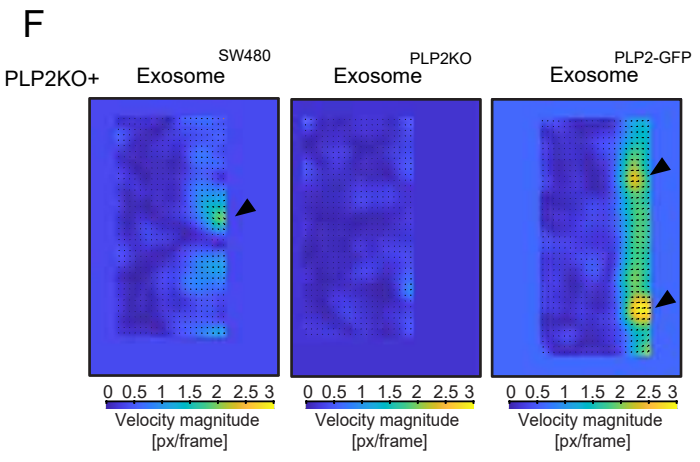

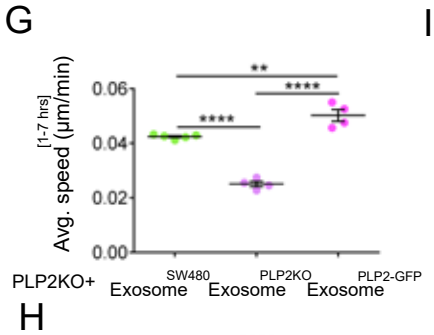

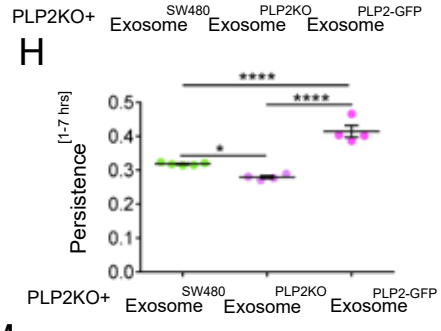

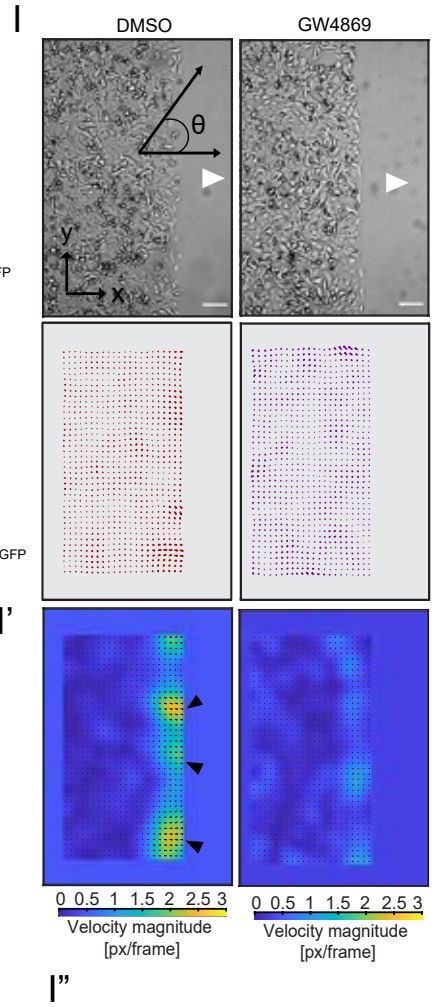

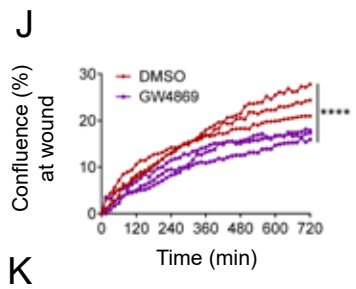

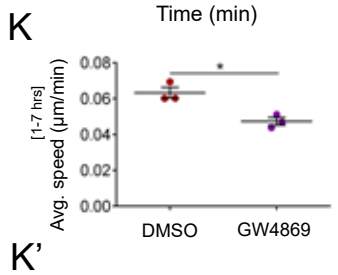

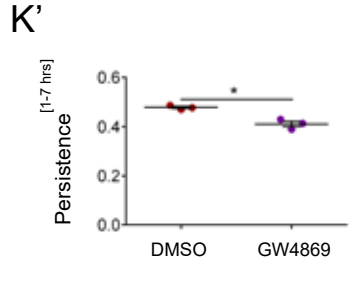

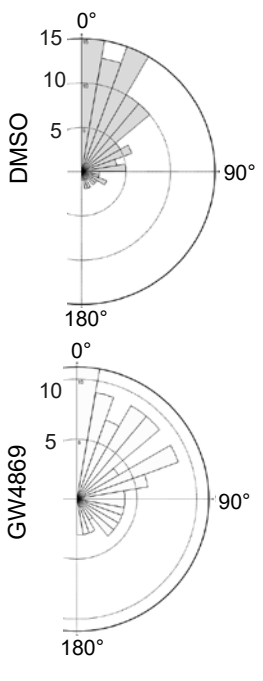

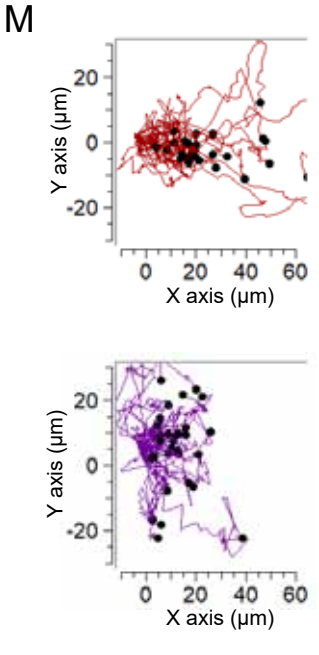

Fig. S3. Exosomal PLP2 contributes to collective cell migration: A) Endogenous PLP2 is secreted and enriched in exosomes purified from SW480 cells. SW480 whole cell lysate (WCL) and density gradient purified exosomes (DG Exosome) were lysed to extract total proteins and immunoblotted with PLP2 antibody along with positive (Alix and Tsg101) and negative (GM130 and Nup62) markers for exosomal proteins. Vinculin was used as a loading control. GW4869 treatment reduced the PLP2 protein level in the exosome fraction. A') The endogenous PLP2 protein level remained unchanged upon GW4869 treatment (5μM for 48 hrs). Actin was used as a loading control. WCL: Whole cell lysate. B) Nanosight quantification of density gradient purified exosomes from cell culture supernatants of SW480 cells with and without GW4869 treatment or stably overexpressing PLP2-GFP. Data represented as mean± SEM from five, five, and four independent experiments, respectively. C) Density gradient purified exosomes isolated from PLP2KO cells showed absence of PLP2 in the exosome fractions positive for Tsg101 and negative for GM130 and nucleoporin (Nup62). Exosomes isolated from SW480 cells was used as a positive control. Tubulin was used as a loading control. D) Exosome$^{PLP2\text{-}GFP}$ treated PLP2KO cells showed distinct intracellular PLP2-GFP localization at 16 hrs post-treatment. D') Exosome$^{PLP2\text{-}GFP}$ treated PLP2KO cells were incubated at 37°C for 16 hrs post-treatment. Cells were then harvested and lysed to extract total protein and immunoblotted with the GFP antibody for the detection of PLP2-GFP. Whole-cell lysate from cells stably overexpressing PLP2-GFP was used as a positive control. Vinculin was used as the loading control. Samples from two replicate experiments were shown. E) to H) Wound scratch assay performed on PLP2KO cells treated with exosome^{SW480}, exosome^{PLP2KO} and exosome$^{PLP2\text{-}GFP}$. E) and F) PIV analysis.

E) Average collective speed in the entire cell layer measured between 1 to 7 hrs post-wound. Data represented as scattered plots showing mean±SEM from five, four and four independent experiments respectively. F) Velocity heatmaps (1 pixel = 0.585 μm; 1 frame= 15 mins; yellow color indicates high-speed zones, pointed with black arrows). G) and H) Track analysis from individual cells tracked from the first four layers of the progressing cell sheet. G) Average speed and H) Persistence of cells measured between 1 to 7 hrs post-wound. For G) and H) Data represented as scatter plots with mean±SEM; (N=5, n=40+38+41+34+45= 198 for PLP2KO cells+ exosome^{SW480}; N=4, n=65+47+71+76=259 for PLP2KO cells+ exosome^{PLP2KO} and N=4, n=100+91+113+118=422 for PLP2KO cells+ exosome$^{PLP2\text{-}GFP}$). I) to M) Wound scratch assay performed on SW480 cells treated with DMSO or GW4869. I) to I") PIV analysis. I) Phase-contrast images and corresponding velocity fields 7 hrs post-wound. I') Velocity heatmaps (1 pixel = 0.585 μm; 1 frame= 15 mins; yellow color indicates high-speed zones, pointed with black arrows) and I") Average collective speed in the entire cell layer measured between 1 to 7 hrs post-wound. Data represented as scattered plots showing mean±SEM (N=3). J) Confluence of cells within the wound area measured between 1 to 12 hrs post-wound. Data represented as individual replicates of three independent experiments. K) to M) Track analysis.

K) Average speed and K') Persistence of cells measured between 1 to 7 hrs post-wound. For K) and K') Data represented as scatter plots with mean±SEM; (N=3, n=78+75+96=249 for DMSO treated and N=3, n=31+60 +24=115 for GW4869 treated cells). L) Rose plots of angle trajectories. The magnitude of each bar shows the fraction of cells within the indicated angle trajectory. n= 317 for DMSO treated and n=316 for GW4869 treated cells from four and six independent experiments respectively. M) Trajectories of 30 representative cells measured over 12 hrs. All panels: N= number of experiments, n= number of tracks. Statistical significance was calculated using one way ANOVA (For E, G and H) and an unpaired two-tailed t-test (For B, I", K and K'). *, $P<0.05$; **, $P<0.005$; ***, $P<0.0005$; ****, $P<0.0001$. Scale bars D) 15 μm; I) 100 μm.

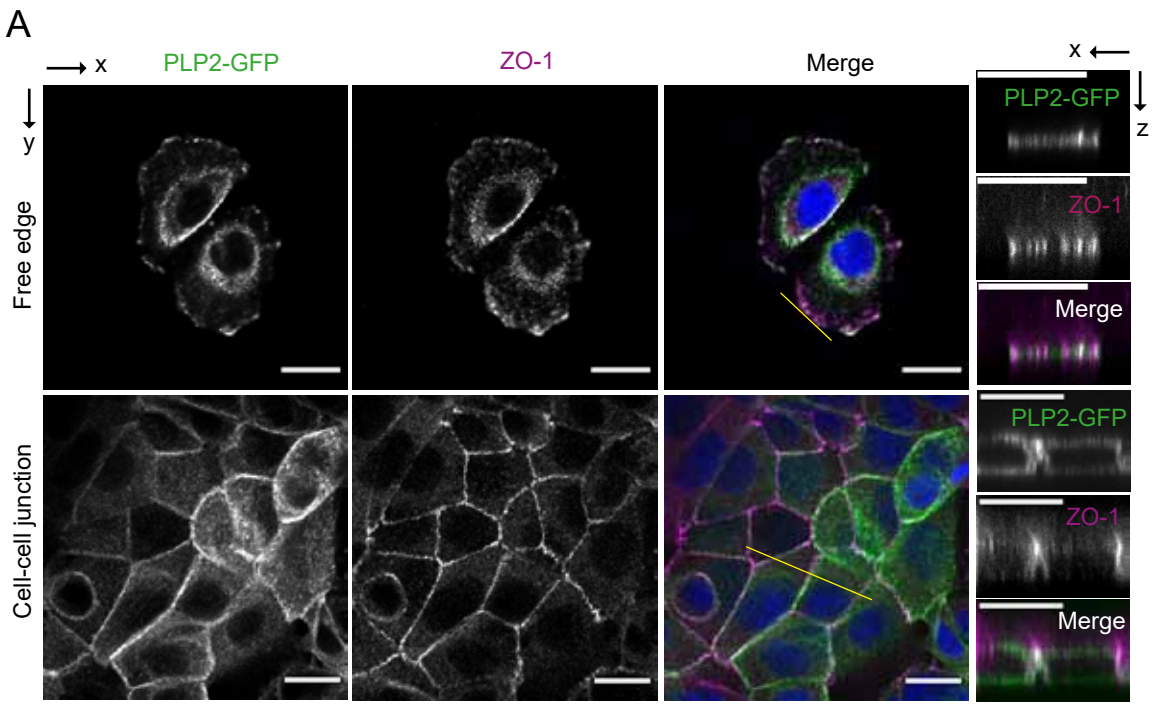

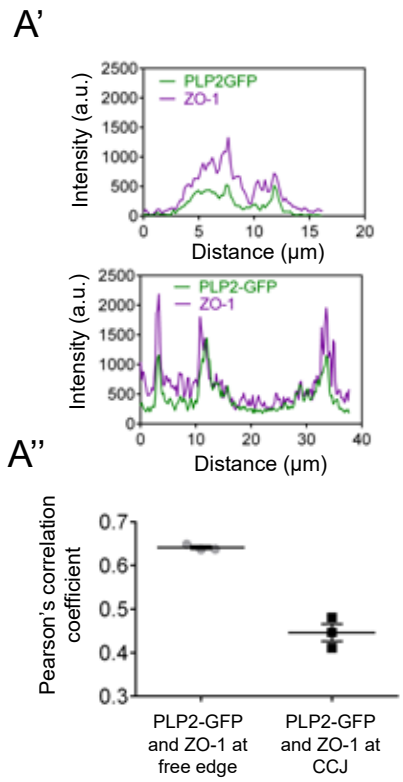

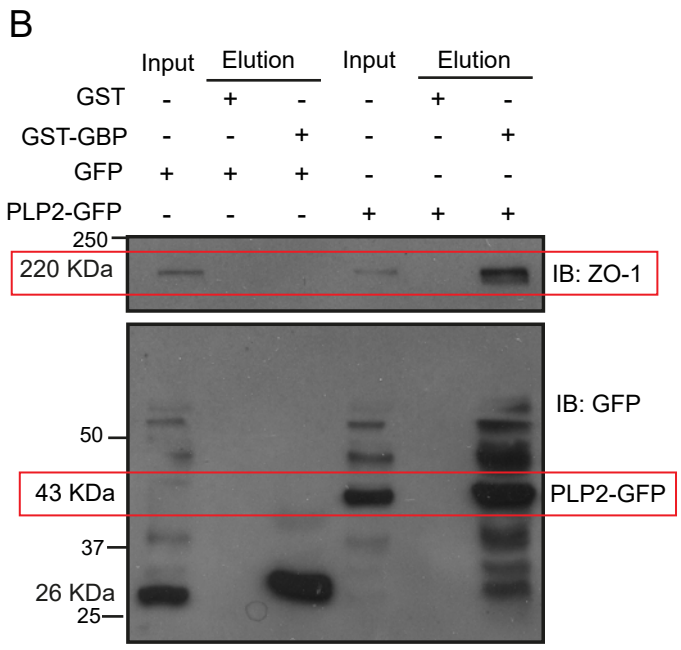

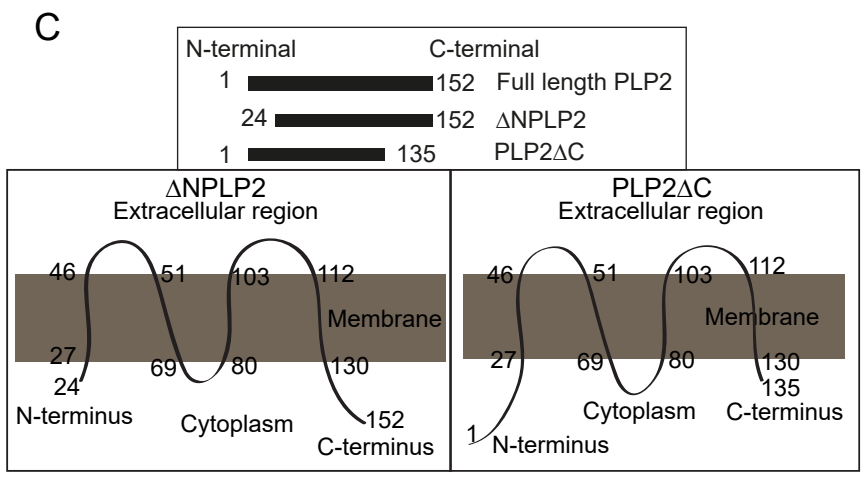

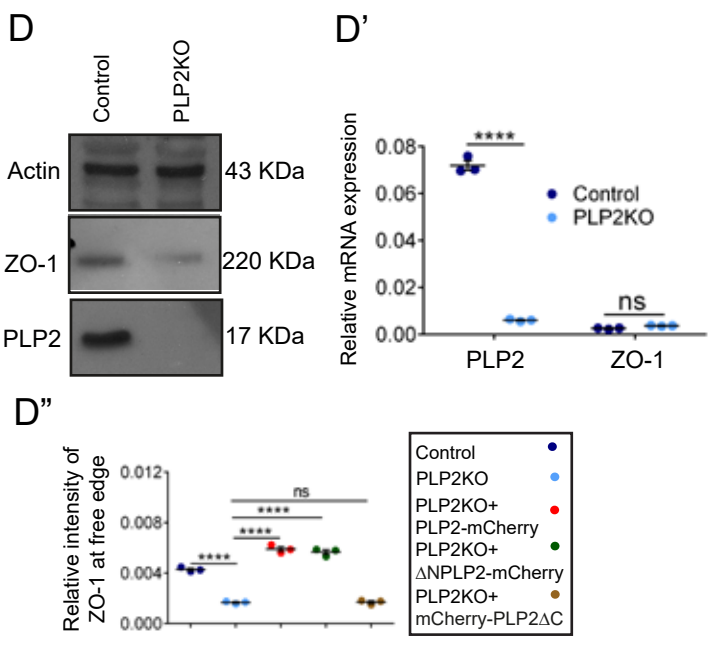

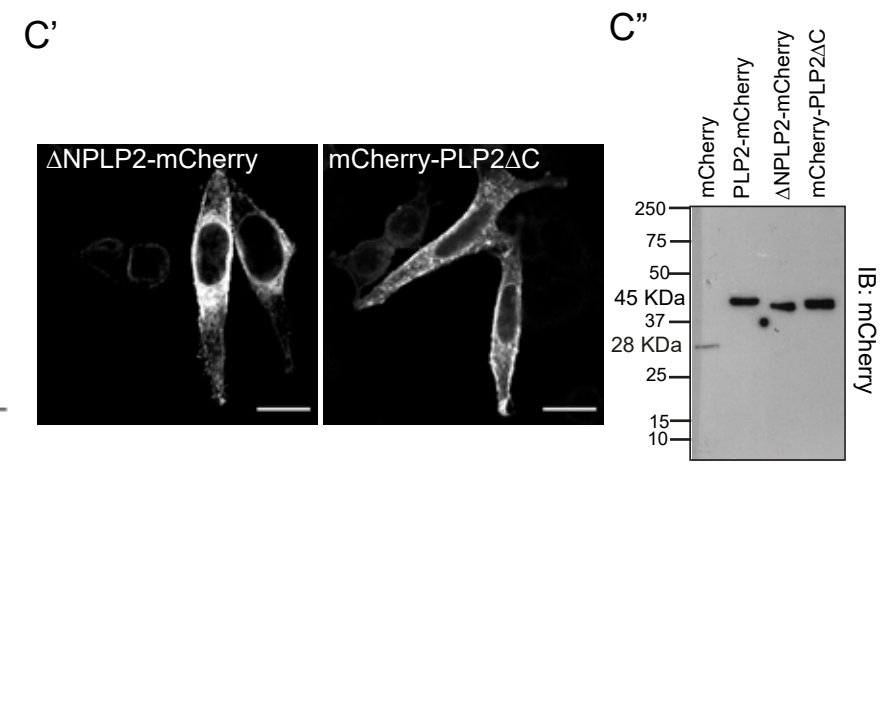

Fig. S4. PLP2 associates with ZO-1 via the C terminal cytoplasmic tail of PLP2. A) Colocalization of PLP2-GFP and ZO-1 at the free edge protrusions (upper panels) and cell-cell junctions (lower panels). Images were captured along the x-y as well as x-z direction. A') The intensity plots of the fluorescent intensity (y-axis) against distance (x-axis) represent the overlap between channels that interprets colocalization of PLP2-GFP and ZO-1 at respective sites. A") The colocalization between PLP2-GFP and ZO-1 at the cell-free edge and at the cell-cell junction was quantified by Pearson's correlation coefficient from three independent experiments (N=3) and represented as a scatter plot (means±SEM); cells quantified n=78 (24+27+27) for free edge and n=131 (43+41+47) cells for cell-cell junction. B) GFP binding protein (GBP) pull-down assay (Modified immunoprecipitation approach): Cleared lysates from SW480 cells overexpressing GFP and PLP2-GFP were incubated with GST or GST-GBP bound to glutathione-coupled agarose beads for 2 hrs. Beads were then washed three times with 1X PBS. The bound proteins were eluted from the beads by addition of SDS sample loading buffer, resolved on 8% SDS-PAGE and immunoblotted using ZO-1 antibody (Upper lanes) and anti-GFP antibody (lower lanes). 10% of the whole-cell lysates were used as inputs. GST-GBP successfully pull down PLP2-GFP along with ZO-1 that associates with PLP2-GFP in the cellular context. C) Protein length and topology cartoon of ΔNPLP2 and PLP2ΔC. C') Membrane localization of ΔNPLP2-mCherry and mCherry-PLP2ΔC. C") Total protein extracts from cells overexpressing mCherry, PLP2-mCherry, ΔNPLP2-mCherry and mCherry-PLP2ΔC were immunoblotted against mCherry antibody to detect the respective protein levels of the overexpressed proteins. D) Protein level of ZO-1 was depleted in PLP2KO cells. D') The expression level of PLP2 and ZO-1 in the indicated cells, normalized to the expression level of GAPDH. Data represented as scatter plots showing means± SEM from three independent experiments. D") Relative peripheral intensity of ZO-1 at the free edge compared to total frame intensity. Data represented as means± SEM from three independent experiments (N=3) measured over 412 (133+128+151), 466 (143+144+179), 414 (153+126+135), 321 (104+109+108) and 425 (145+129+151) cells for control, PLP2KO and PLP2KO cells overexpressing PLP2-mCherry, ΔNPLP2-mCherry and mCherry-PLP2ΔC respectively. All panels: N= number of experiments, n= number of cells. Statistical significance was calculated using paired t test (D') or one way ANOVA (For D"). ****, P<0.0001, ns=non-significant. Scale-bars A) and C') 15 µm.

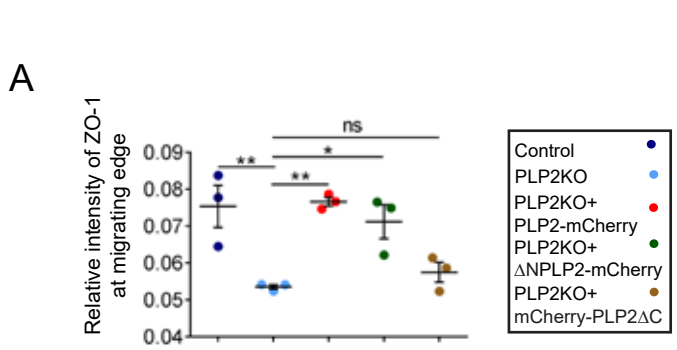

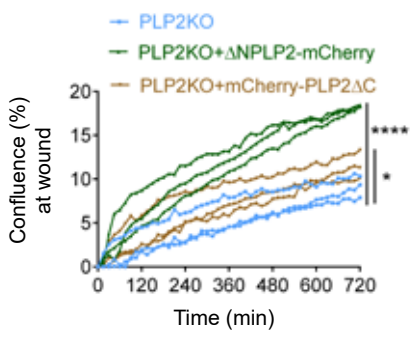

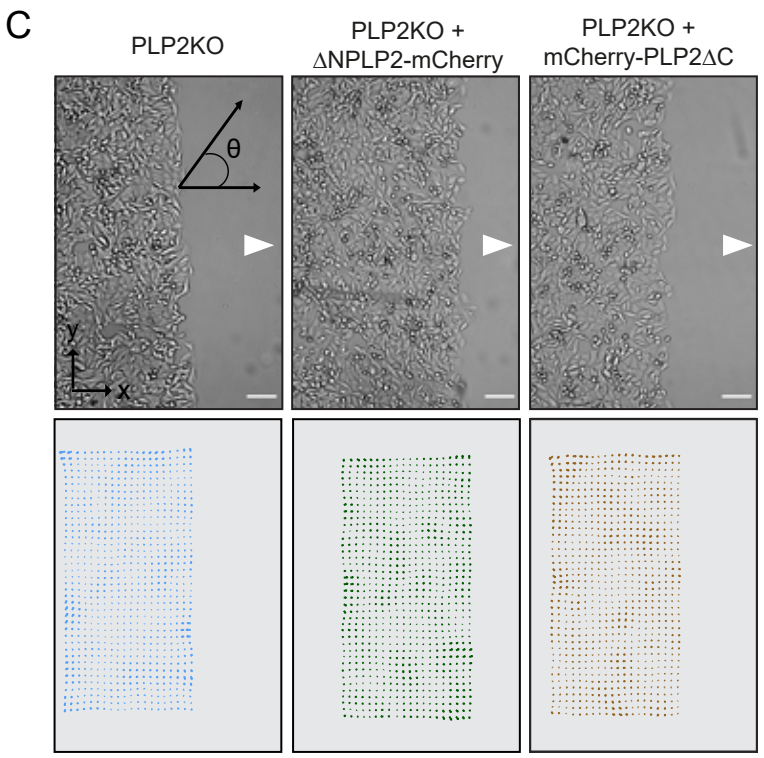

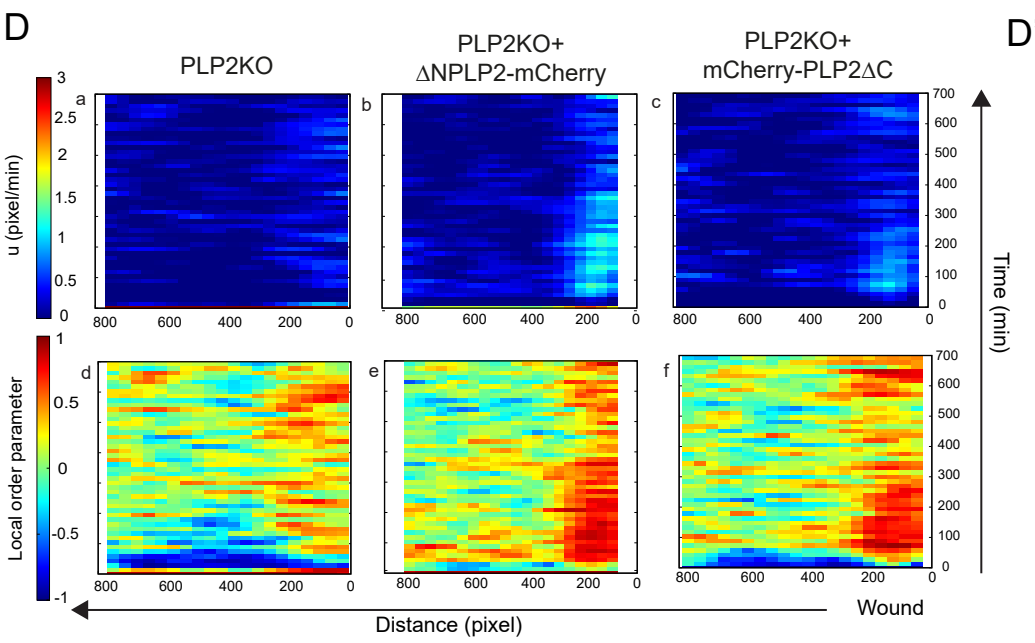

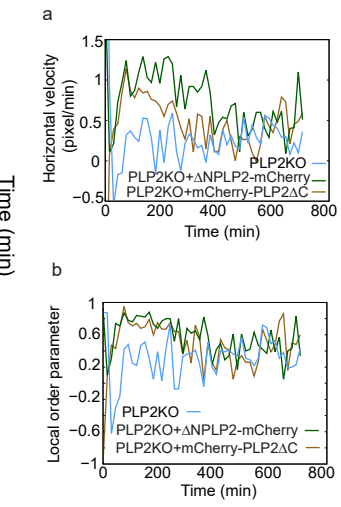

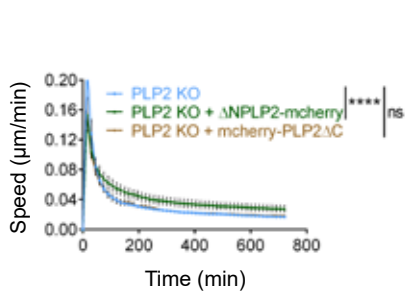

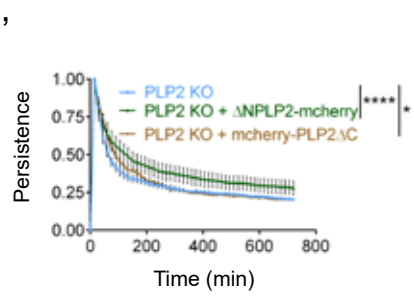

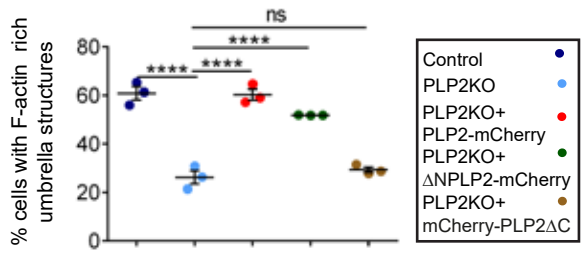

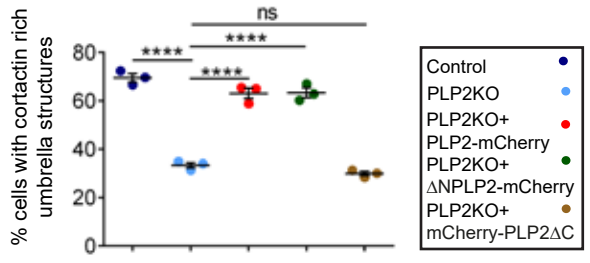

Fig. S5. PLP2-ZO-1 association contributes to PLP2 mediated collective cell migration. A) Relative peripheral intensity of ZO-1 at the leading edge during 4th hr of CCM, compared to total frame intensity. Data represented as means± SEM from three independent experiments (N=3) measured over 245 (72+81 +92), 286 (92+98+96), 237 (83+88+66), 266 (85+98+83) and 287 (81+112+94) cells for control, PLP2KO and PLP2KO cells overexpressing PLP2-mCherry, ΔNPLP2-mCherry and mCherry-PLP2ΔC respectively. B) to E') Wound scratch assay performed on PLP2KO, PLP2KO cells overexpressing ΔNPLP2-mCherry or mCherry-PLP2ΔC. B) The confluence of cells within the wound area measured between 1 to 12 hrs post-wound. Data represented as individual replicates of three independent experiments. C) Phase-contrast images (white arrowhead indicates the direction of migration) and corresponding velocity fields at 7 hrs post-wound. D) Kymographs showing spatiotemporal dynamics of (a,b,c) horizontal velocity (u) (pixel/ min), and (d,e,f) local order parameter. 1 pixel=0.586 µm. The distance at the wound edge was taken as zero with gradual increment towards (-) x-direction (refer to Fig. 2B). D') Time dependence of (a) horizontal velocity component (pixel/min) and (b) local order parameter at a given X averaged over Y in respective cells. X= 104 for PLP2KO, 126 for PLP2KO+ΔNPLP2-mCherry, 124 for PLP2KO+mCherry-PLP2ΔC. E) & E') Track analysis from individual cells tracked from the first four layers of the progressing cell sheet. E) Speed & E') Persistence over 12 hrs post-wound. Data represented as mean±SEM from four, six and three independent experiments performed on PLP2KO, PLP2KO+ΔNPLP2-mCherry and PLP2KO +mCherry-PLP2ΔC cells respectively. F) Quantification on the number of cells from the first row, containing F-actin rich lamellipodia (umbrella) like structures. Data represented as mean±SEM of percentages from three independent experiments (N=3) measured over 206 (59+106+41), 228 (92+78+58), 212 (91+90+31), 259 (127+89+43) and 182 (61+78+43) cells for control, PLP2KO, and PLP2KO cells overexpressing PLP2-mCherry, ΔNPLP2-mCherry, and mCherry-PLP2ΔC respectively. G) Quantification on the number of cells from the first row, containing cortactin rich lamellipodia (umbrella) like structures. Data represented as mean±SEM of percentages from three independent experiments (N=3) measured over 312 (119+113+80), 399 (132+163+104), 452 (131+199+122), 438 (143+165+130) and 465 (142+198+125) cells for control, PLP2KO, and PLP2KO cells overexpressing PLP2-mCherry, ΔNPLP2-mCherry, and mCherry-PLP2ΔC respectively. All panels: n=number of tracks/ cells. Statistical significance was calculated using one way ANOVA (For A, B, E, E', F and G). *, P<0.05; **, P<0.005; ****, P<0.0001; ns=non-significant. Scale-bars C) 100 µm.

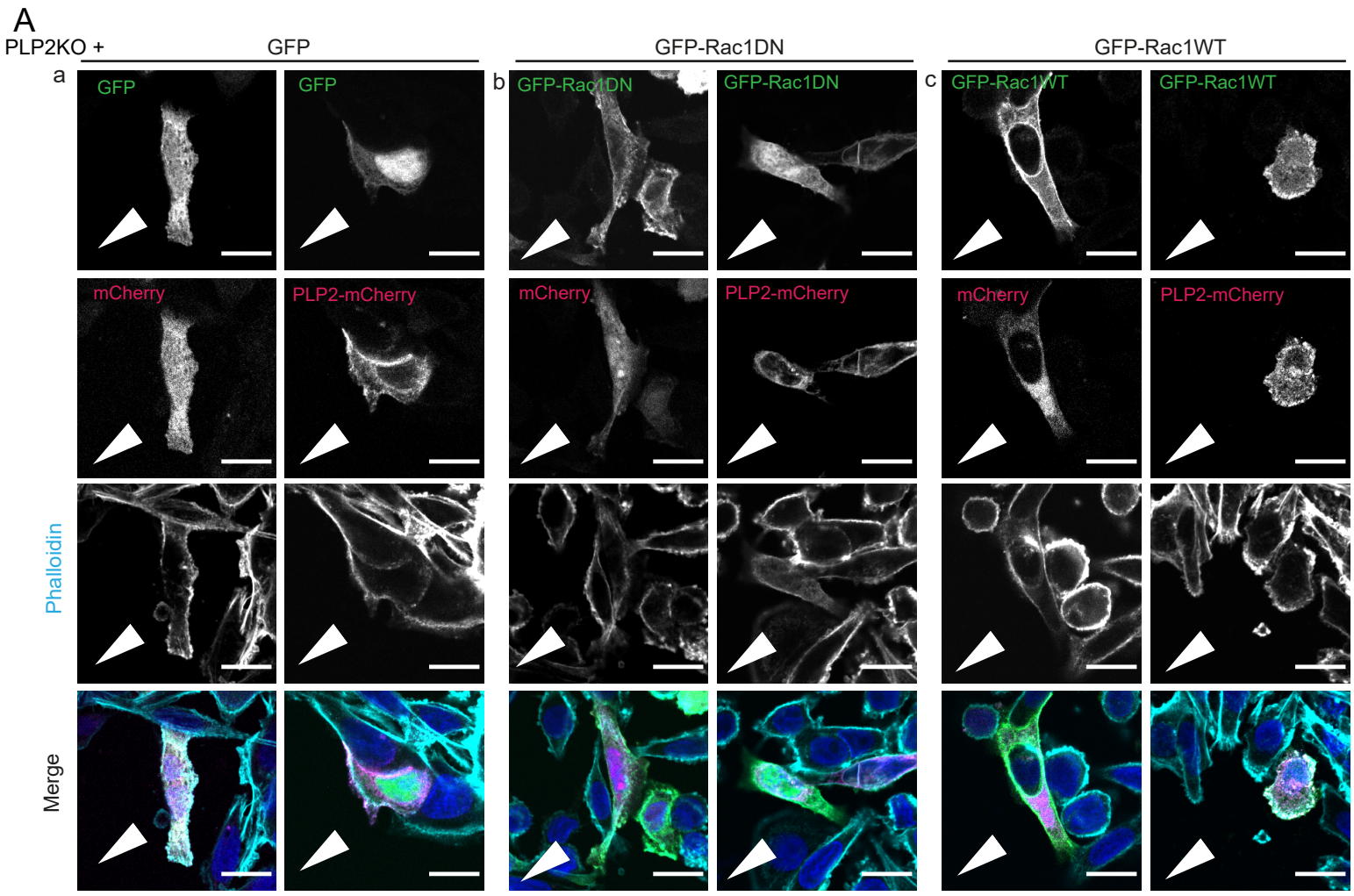

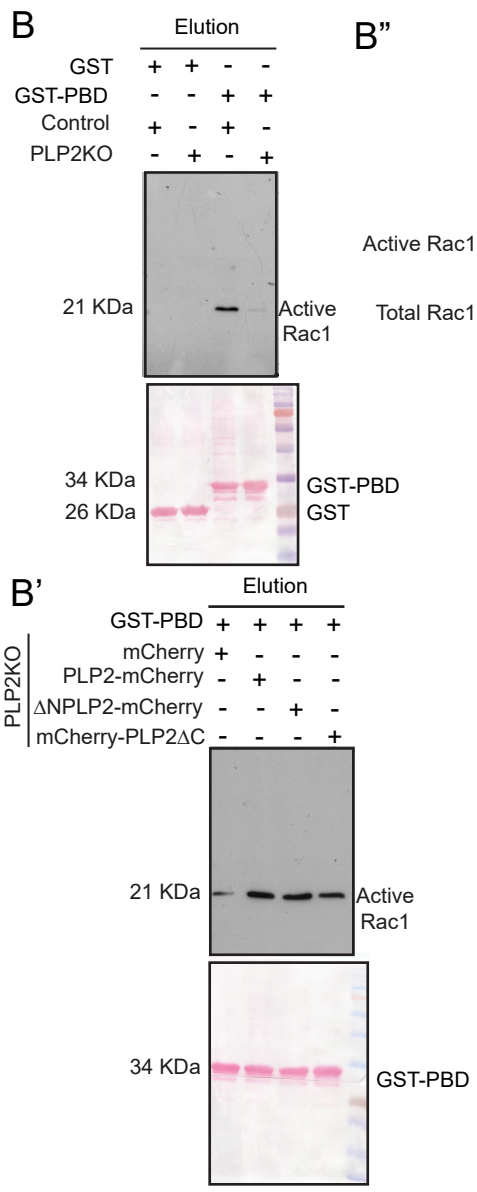

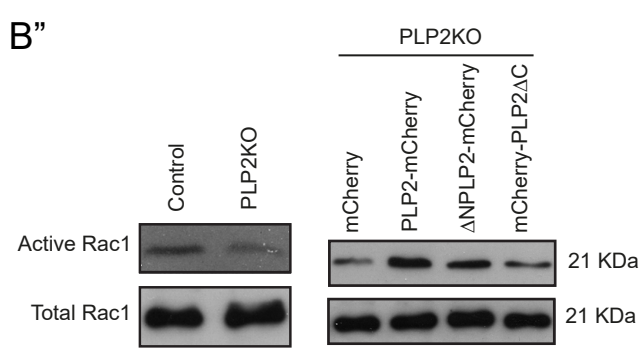

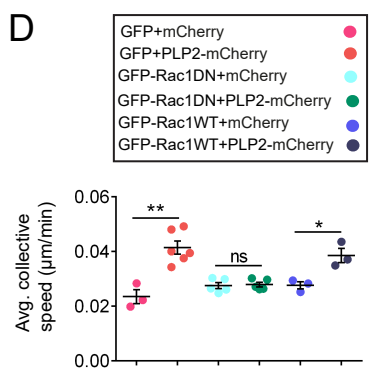

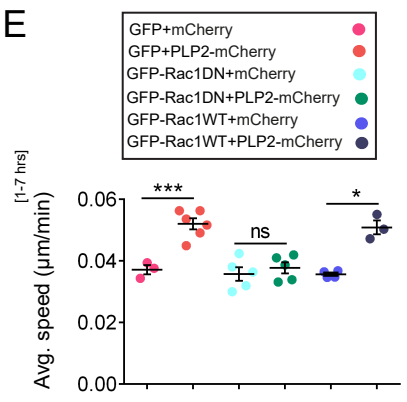

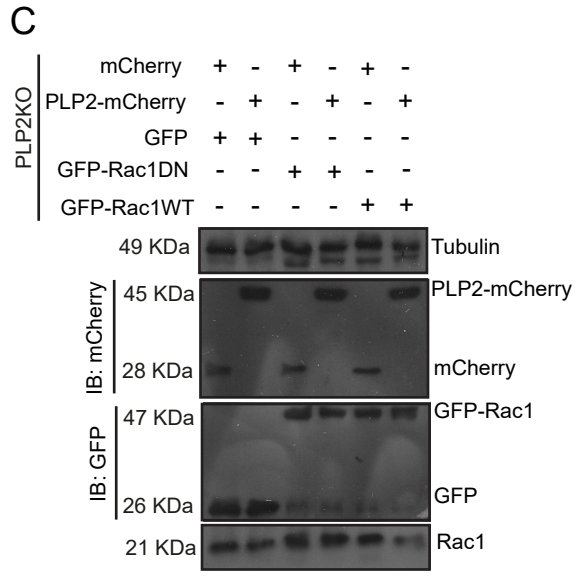

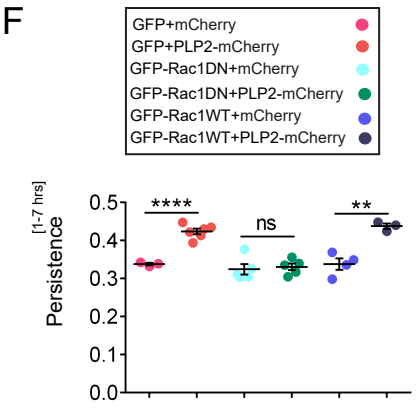

Fig. S6. Rac1 activation contributes to PLP2 mediated CCM. A) F-actin rich umbrella like structures at the leading edge as observed during 4th hour post-wound in PLP2KO cells co-expressing mCherry and GFP/ GFP-Rac1DN/ GFP-Rac1WT or PLP2-mCherry and GFP/ GFP-Rac1DN/ GFP-Rac1WT. B) to B") Rac1 activation assay: Control and PLP2KO (B) and PLP2KO cells overexpressing mCherry, PLP2-mCherry, ΔNPLP2-mCherry or mCherry-PLP2ΔC (B') full blot with bait protein (GST/ GST-PBD) identification by ponceau stain. Reference to main figure 6B and B'. B") Blots for experiment 2 of Rac1 activation assay. C) Protein levels of endogenous Rac1, mCherry, PLP2-mCherry, GFP, GFP-Rac1DN, GFP-Rac1WT in PLP2KO cells co-expressing mCherry and GFP/ GFP-Rac1DN/ GFP-Rac1WT or PLP2-mCherry and GFP/ GFP-Rac1DN/ GFP-Rac1WT. D) to F) wound scratch assay performed on PLP2KO cells co-expressing mCherry and GFP/ GFP-Rac1DN/ GFP-Rac1WT or PLP2-mCherry and GFP/ GFP-Rac1DN/ GFP-Rac1WT. D) PIV Analysis: Average collective speed measured between 1 to 7 hrs post-wound. Data represented as mean±SEM from three, five and three independent experiments for PLP2KO cells co-expressing mCherry and GFP/ GFP-Rac1DN/ GFP-Rac1WT respectively and six, five and three independent experiments for PLP2KO cells co-expressing PLP2-mCherry and GFP/ GFP-Rac1DN/ GFP-Rac1WT respectively. E) and F) Track analysis. E) Average speed and F) persistence measured between 1 to 7 hrs post-wound. Data represented as scatter plots with mean±SEM for PLP2KO cells co-expressing mCherry and GFP (n=189)/ GFP-Rac1DN (n=532)/ GFP-Rac1WT (n=207) from three, five and four independent experiments respectively and co-expressing PLP2-mCherry and GFP (n=414)/ GFP-Rac1DN (n=315)/ GFP-Rac1WT (n=267) from six, five and three independent experiments respectively. All panels: n= number of tracks/cells. Statistical significance was calculated using an unpaired two-tailed t-test (For D, E and F). ns=non-significant; *, P<0.05; **, P<0.005; ***, P<0.0005; ****, P<0.0001. Scale bars A) 15 μm.

A. Fig. 4A

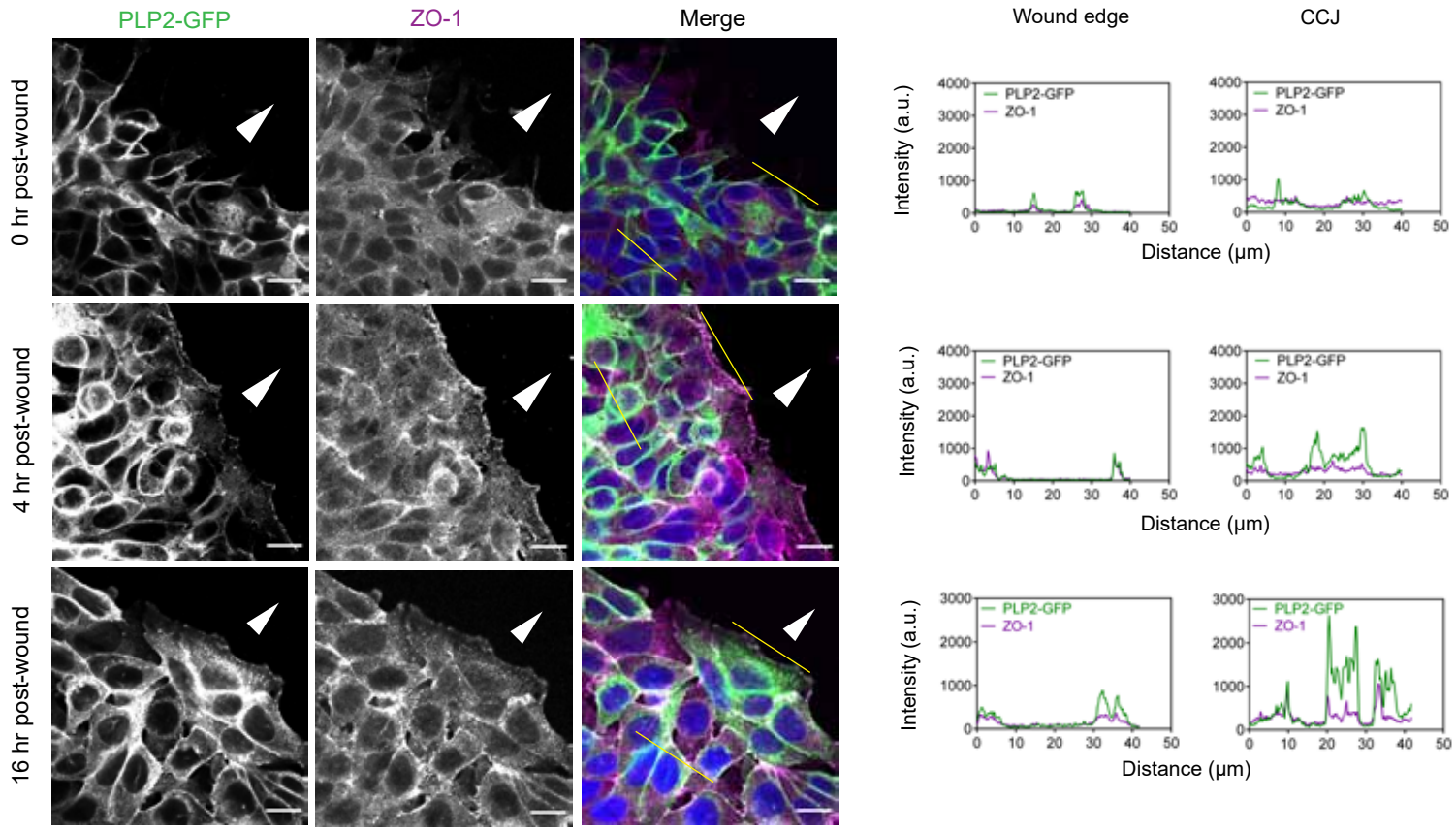

B. Fig. 4E (free edge)

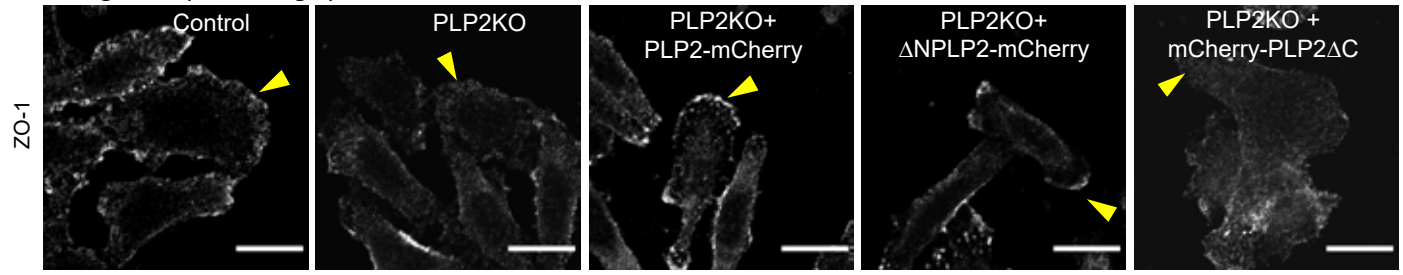

C. Fig. 5A (wound edge)

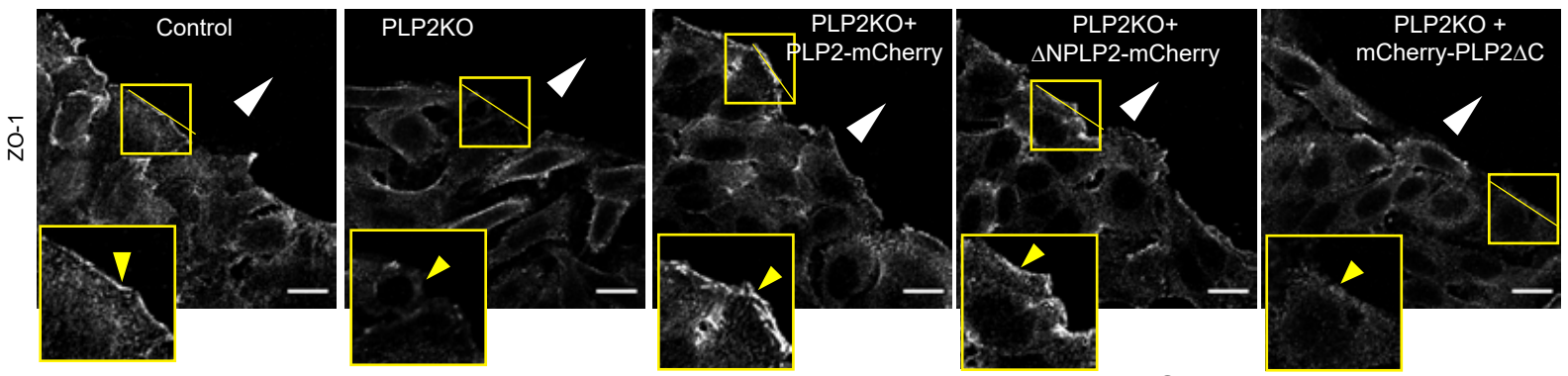

C'

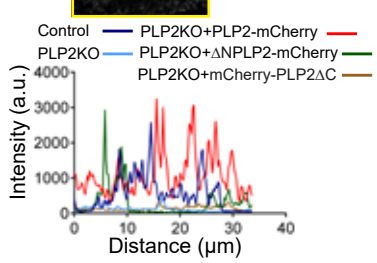

D. Fig. 5G (Umbrella structures)

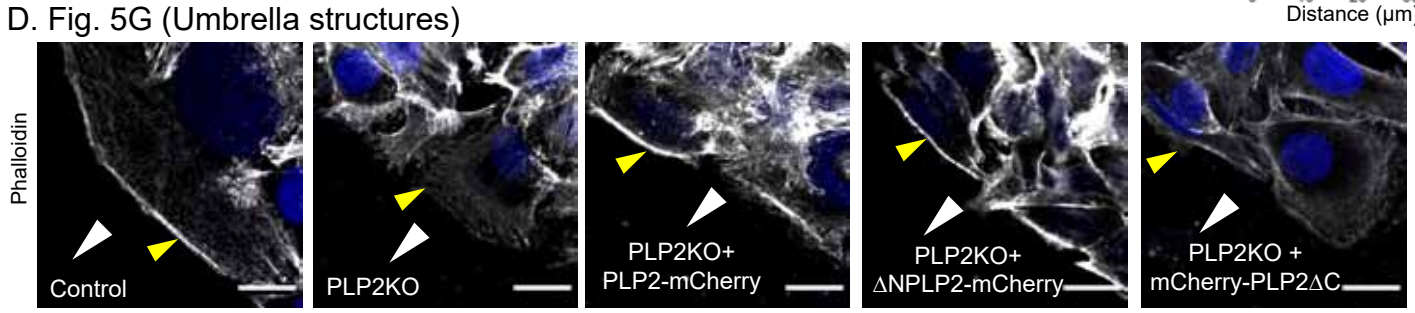

Fig. S7. Additional montages against respective figures. A) Spatiotemporal colocalization of PLP2-GFP and ZO-1 during wound closure; Intensity profile plots represent overlap between two channels; replicate against Fig 4A. B) ZO-1 localization to the free edge of control, PLP2KO and PLP2KO cells overexpressing PLP2-mCherry, ΔNPLP2-mCherry and mCherry-PLP2ΔC cells; replicate against Fig 4Ea. C) ZO-1 localization at the migrating edge during early hours of wound closure (4 hrs post-wound) in control, PLP2KO and PLP2KO cells overexpressing PLP2-mCherry, ΔNPLP2-mCherry and mCherry-PLP2ΔC; insets represent zoomed images of the outline region. The intensity profile plots represent the distribution of ZO-1 protein along the wound edge in respective conditions; replicate against Fig 5A. D) F-actin rich umbrella like structures formed during 4 hrs post-wound in control, PLP2KO and PLP2KO cells overexpressing PLP2-mCherry, ΔNPLP2-mCherry and mCherry-PLP2ΔC at the migrating edges; replicate against Fig. 5G. All panels: Scale bars: 15 μm. White arrowhead indicates direction of migration. Yellow arrowheads point out particular observable phenotypes.

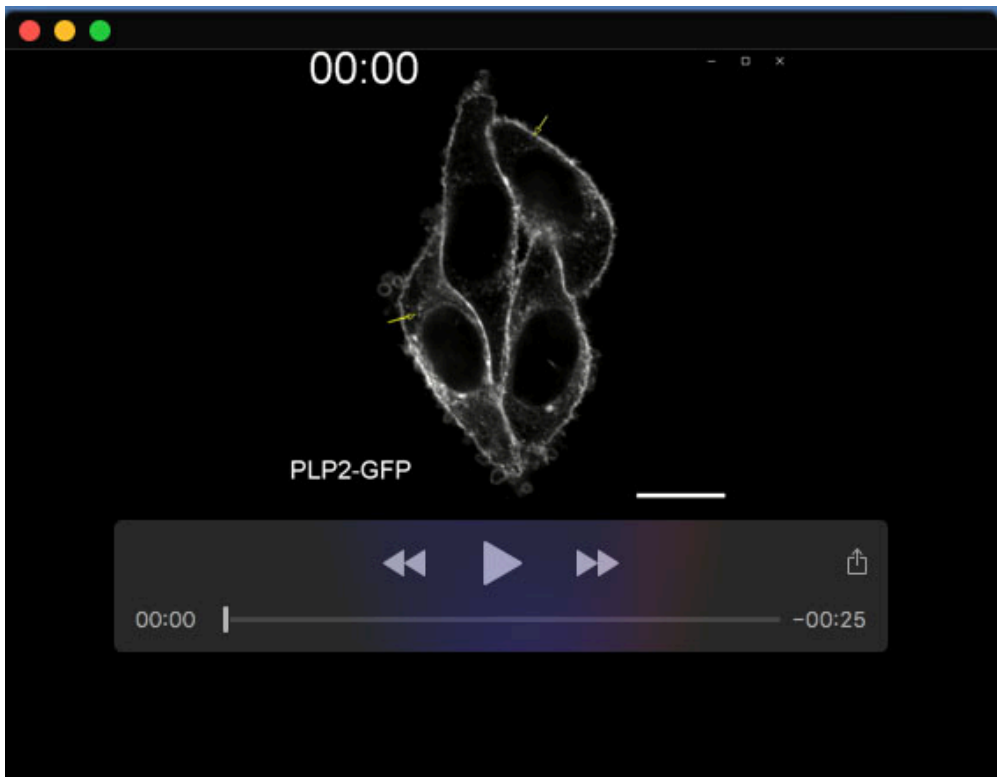

Movie 1. PLP2-GFP localizes to the free edge membrane protrusions, cell-cell junctions and intracellular puncta. 1 frame/ 11 seconds for 3.5 mins. Scale bar: 15 µm. Yellow arrow indicates dynamic membrane structures containing PLP2-GFP.

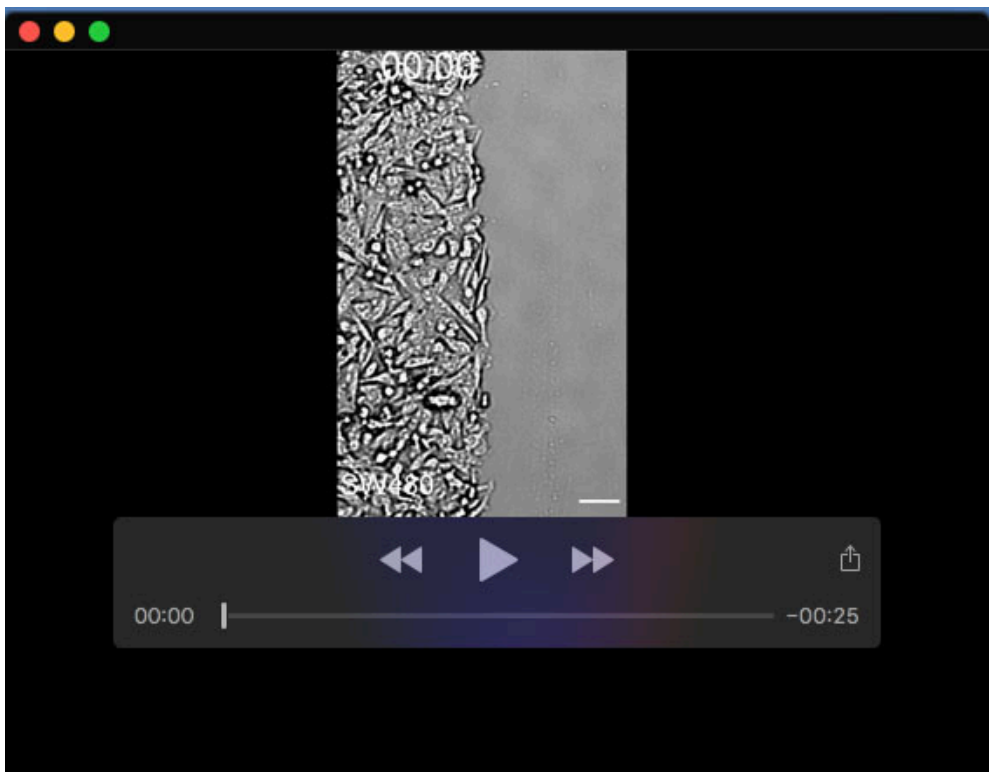

Movie 2. Collective cell migration of wild type SW480 cells. Phase-contrast images of migrating SW480 cells; 1 frame/ 15 mins for 12 hrs. Scale bar: 50 µm.

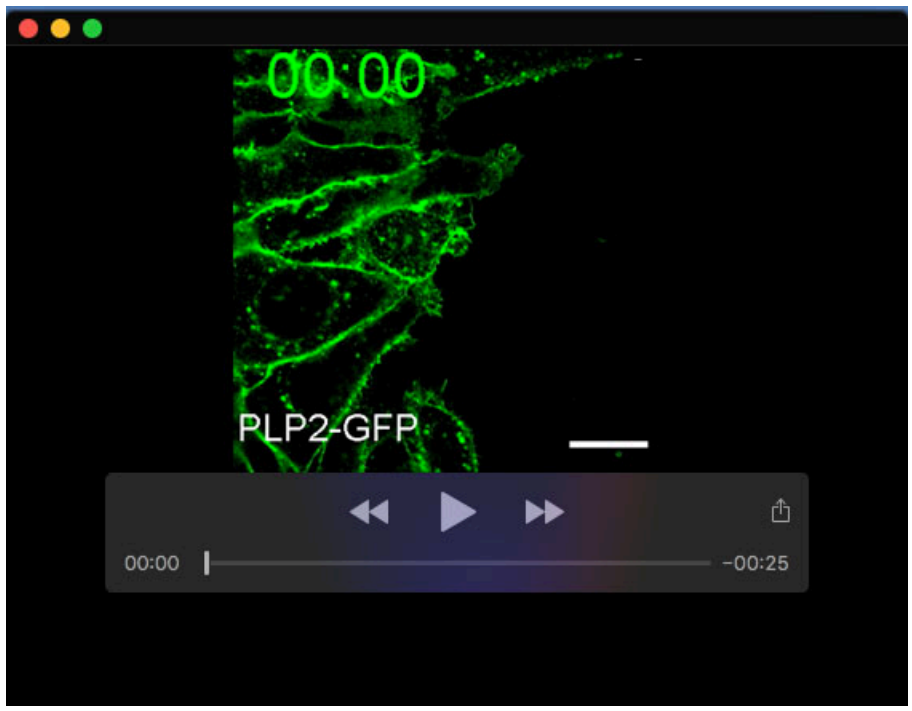

Movie 3. Dynamic localization of PLP2-GFP during migration at 2 hrs post wound creation. 1 frame/ 5 mins for 45 mins. Scale bar: 15 µm.

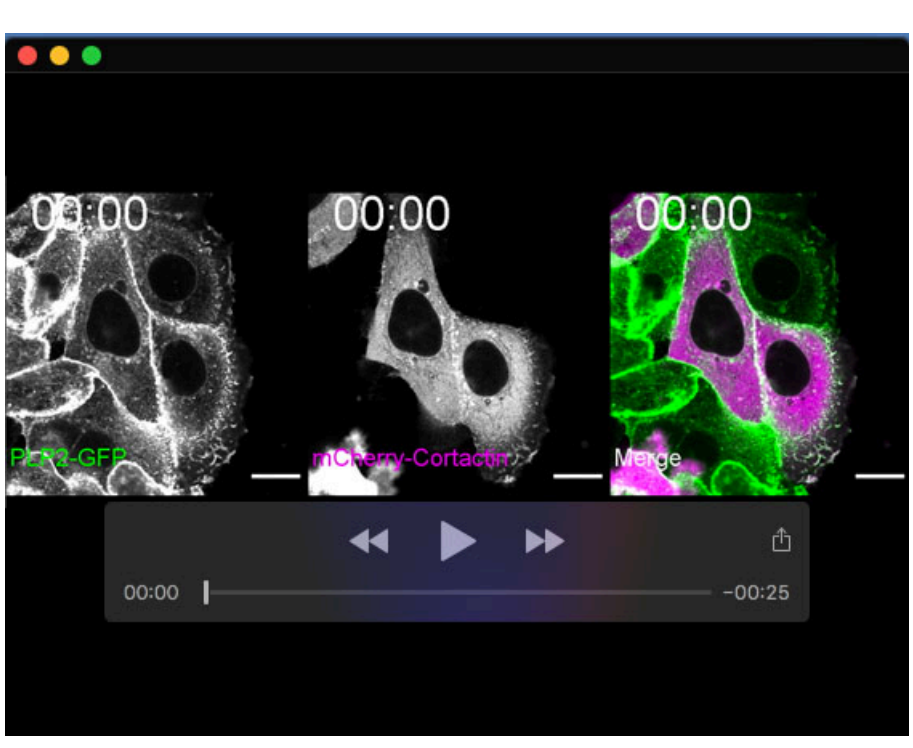

Movie 4. Colocalization dynamics of PLP2-GFP and mCherry-cortactin during migration at 4 hrs post wound creation. 1 frame/ 4 mins for 36 mins. Scale bars: 15 µm.

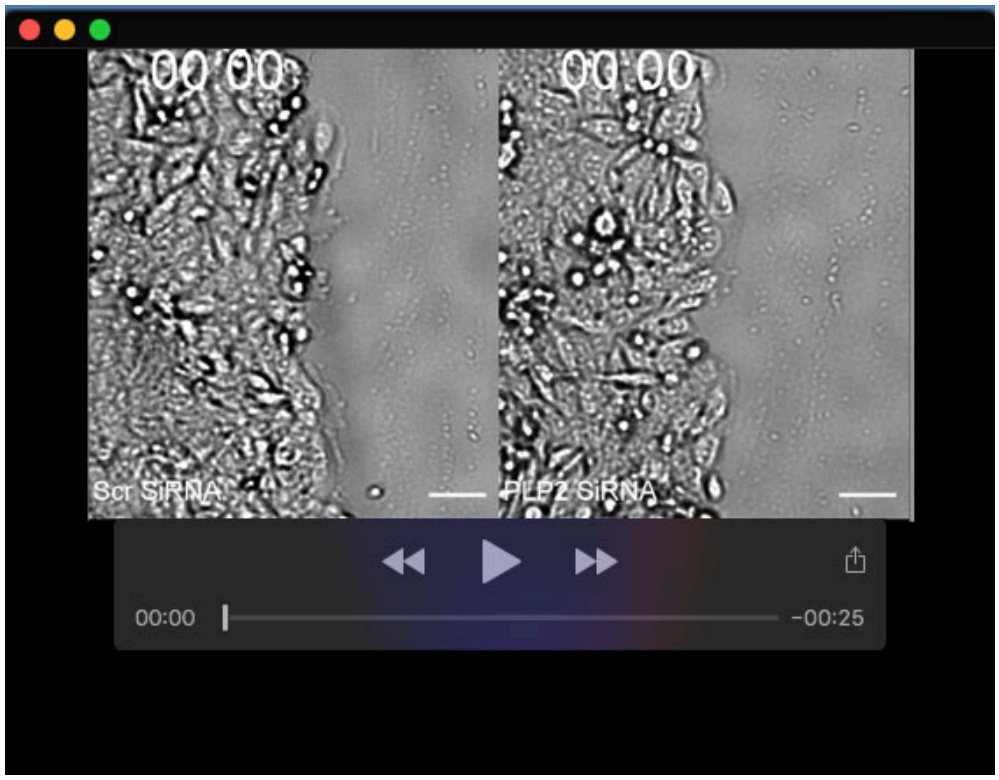

Movie 5. PLP2 depleted cells exhibit slower wound closure. Phase-contrast images of migrating SW480 cells treated with nontargeted (Scr) (left) and PLP2 targeted (right) SiRNA SMARTpool; 1 frame/ 15 mins for 12 hrs. Scale bars: 50 µm.

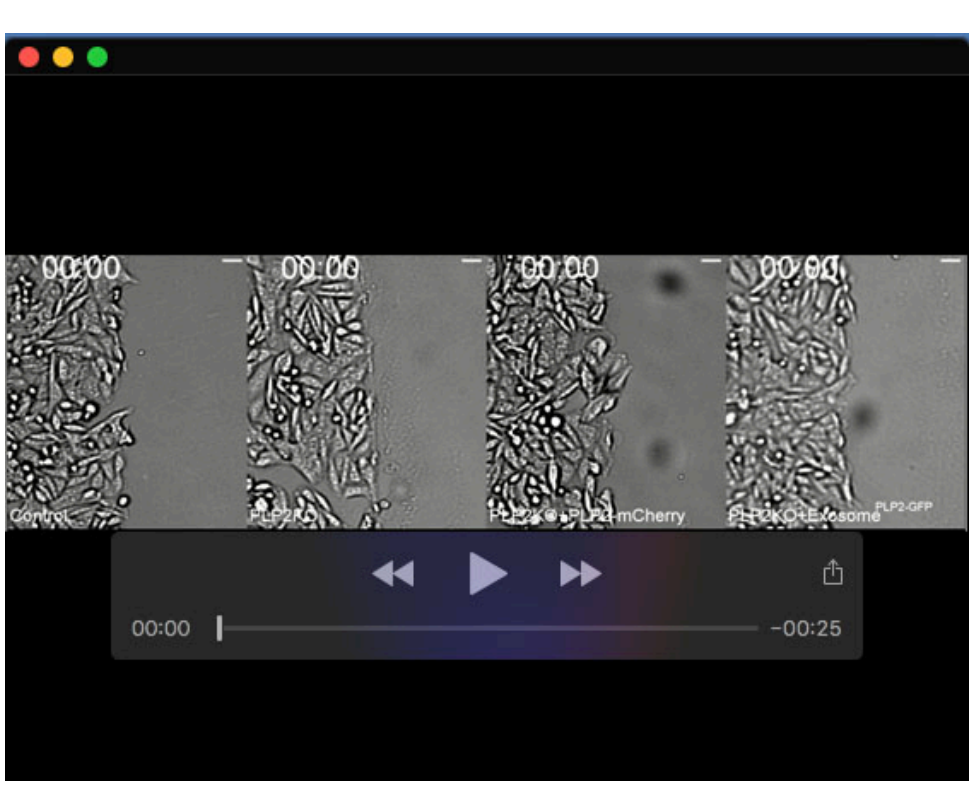

Movie 6. Intracellular and extracellular PLP2 plays a crucial role in collective cell migration. Phase-contrast images of migrating control, PLP2KO, PLP2KO cells overexpressing PLP2-mCherry and PLP2KO cells treated with exosome$^{PLP2\text{-}GFP}$ (respectively from left to right); 1 frame/ 15 mins for 12 hrs. Scale bars: 50 µm.

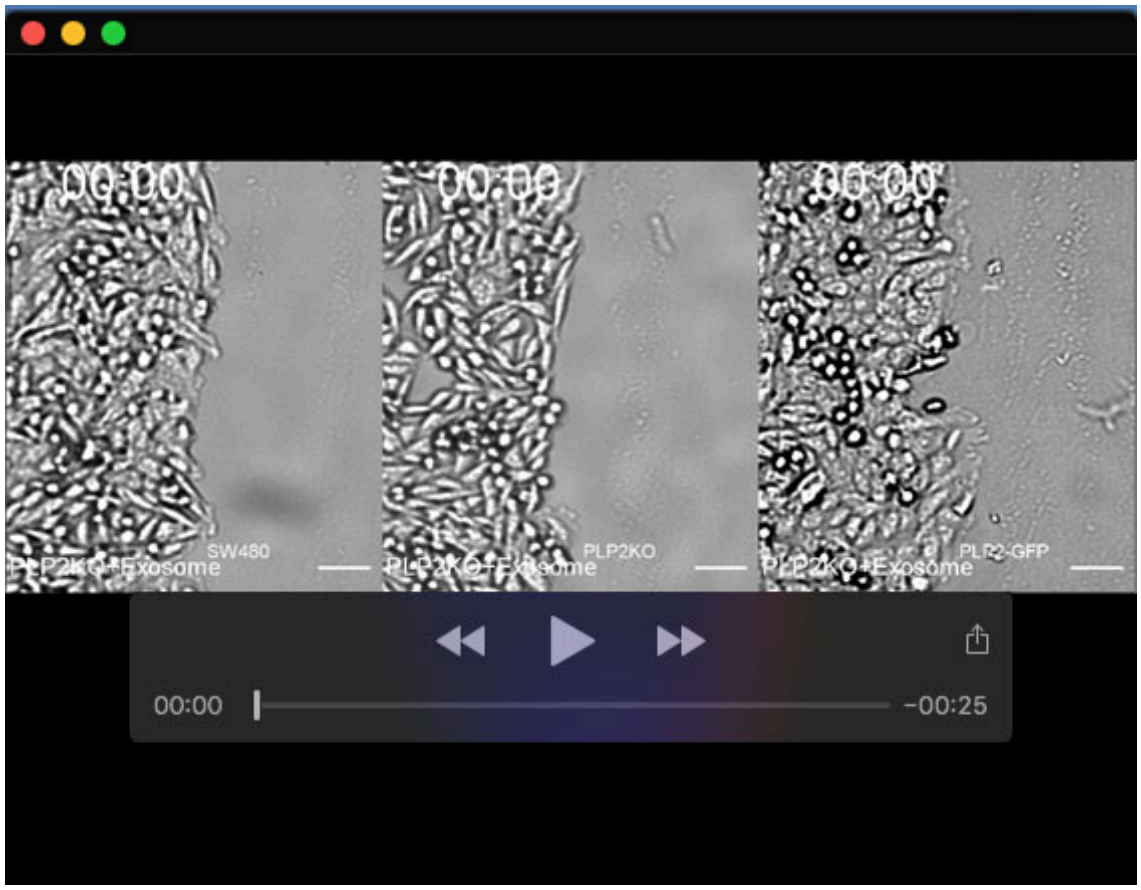

Movie 7. Exosomal PLP2 contributes to the collective migration. Phase-contrast images of migrating PLP2KO cells treated with exosome^{SW480} (left), exosome^{PLP2KO} (middle) and exosome$^{PLP2\text{-}GFP}$ (right); 1 frame/ 15 mins for 12 hrs. Scale bars: 50 µm.

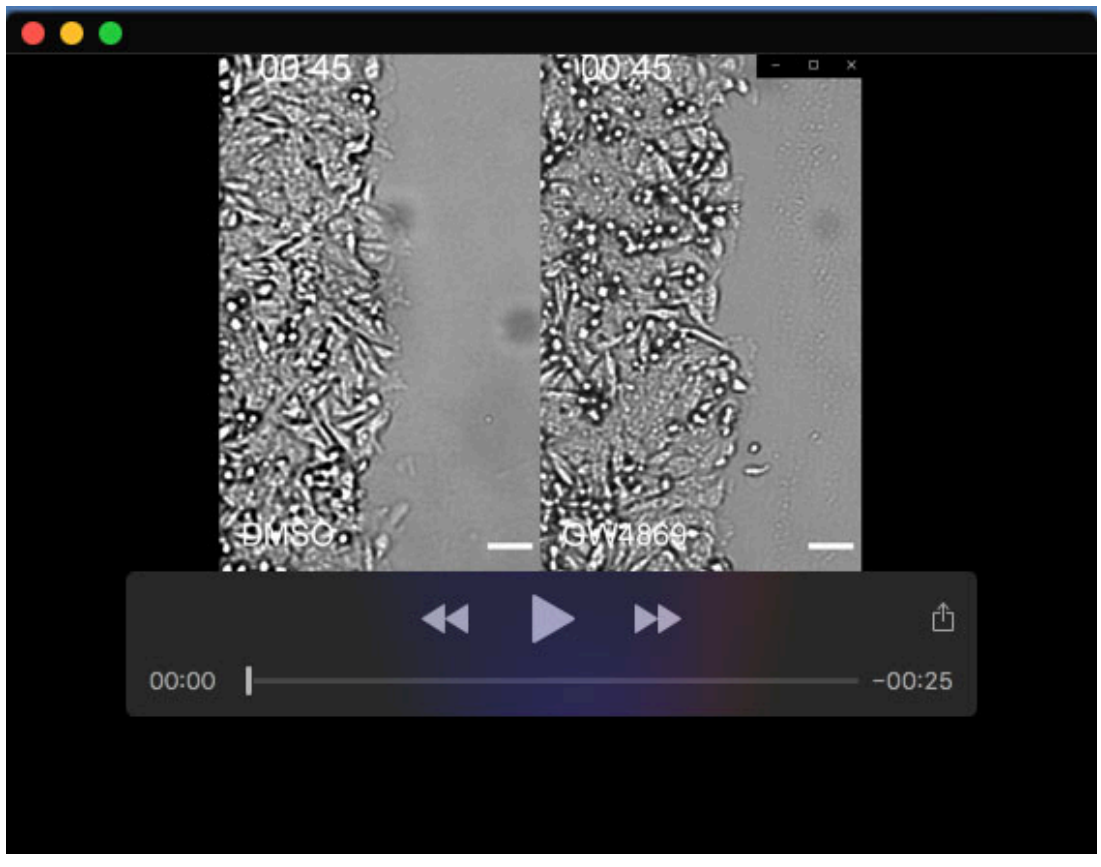

Movie 8. GW4869 treated cells exhibit slower collective cell migration. Phase-contrast images of migrating SW480 cells treated with DMSO (left) and GW4869 (right); 1 frame/ 15 mins for 12 hrs. Scale bars: 50 µm.

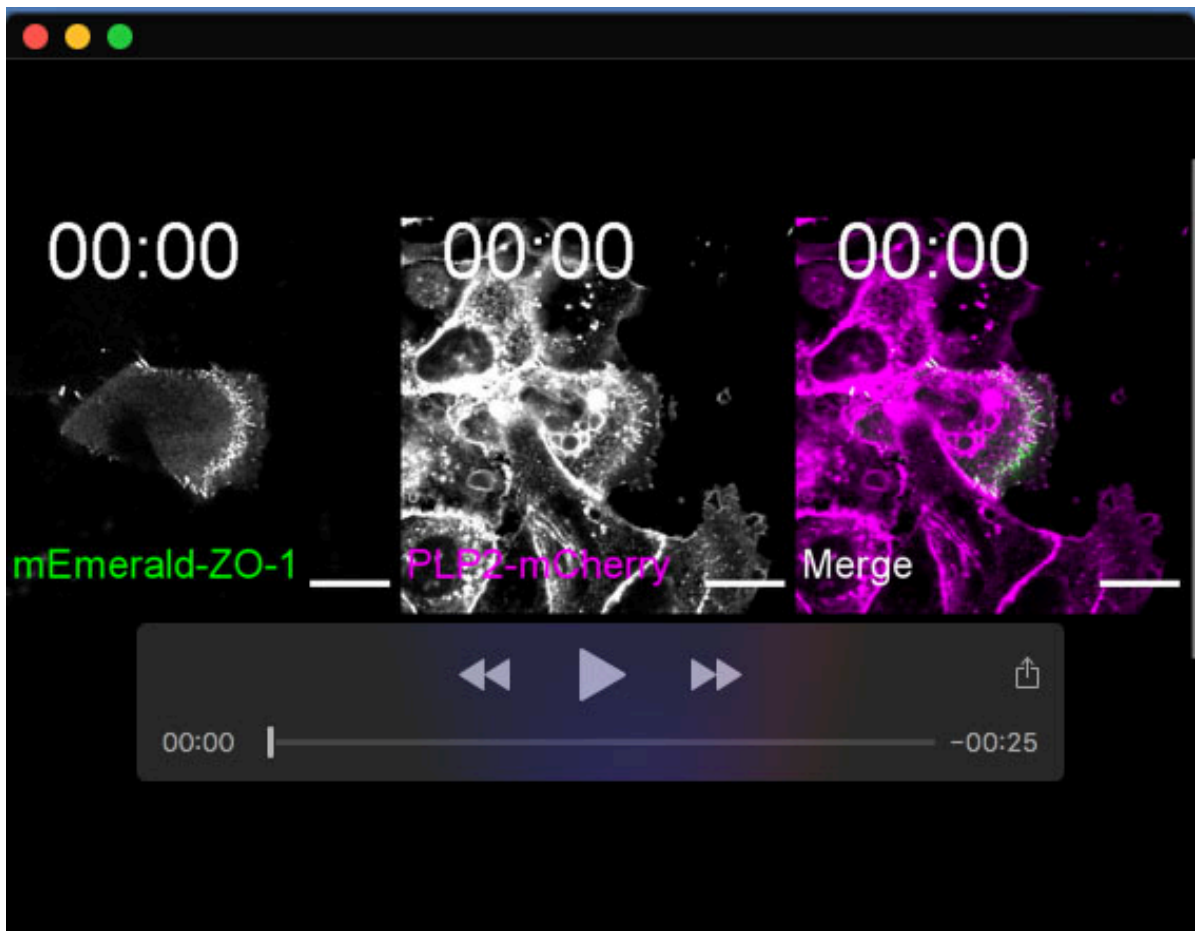

Movie 9. Colocalization dynamics of mEmerald-ZO-1 and PLP2-mCherry during migration at 4 hrs post wound creation. 1 frame/ 4 mins for 36 mins. Scale bars: 15 µm. Yellow arrow indicates dynamic membrane structures where mEmerald-ZO-1 and PLP2-mCherry colocalize.

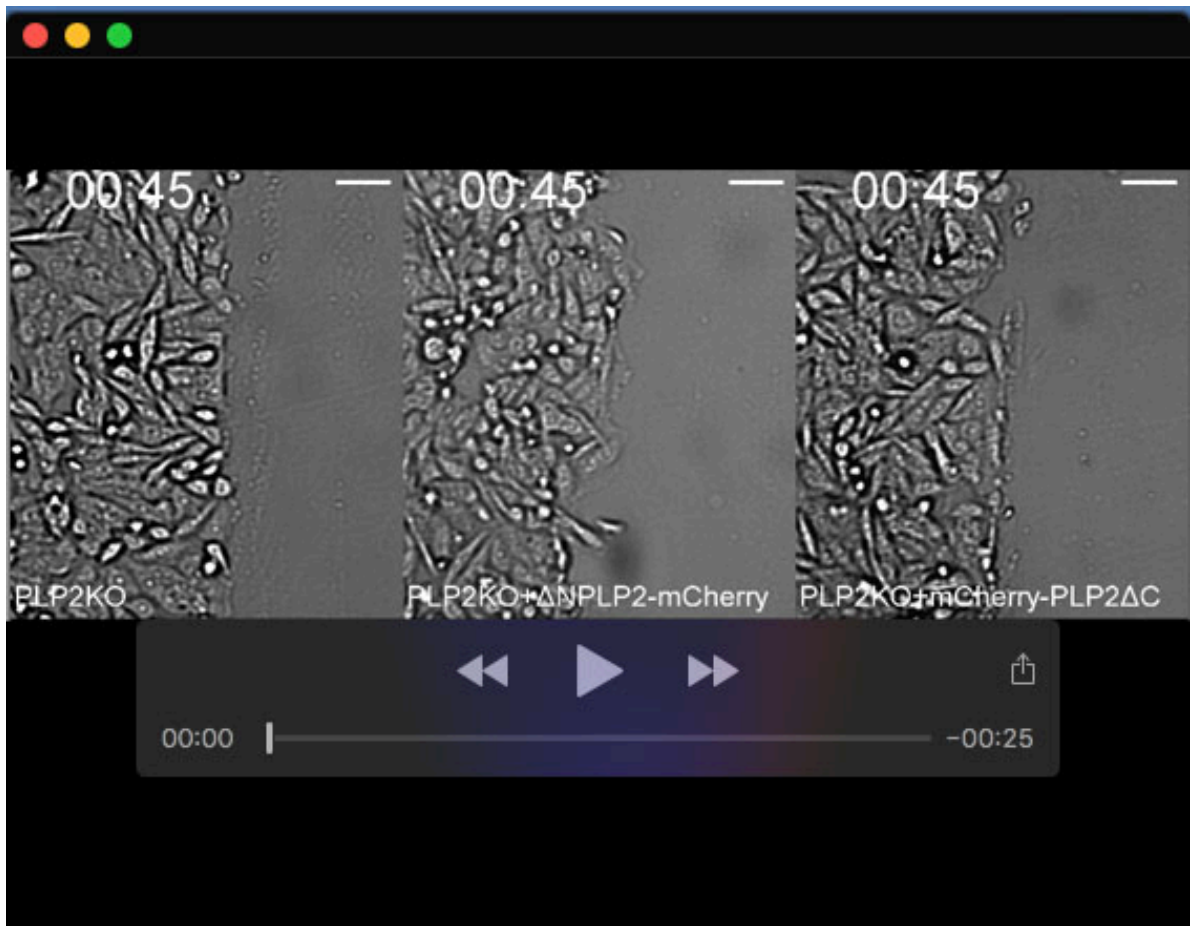

Movie 10. PLP2-ZO-1 association contributes to PLP2 mediated collective cell migration. Phase-contrast images of migrating PLP2KO (left), PLP2KO cells overexpressing ΔNPLP2-mCherry (middle) and mCherry-PLP2ΔC (right); 1 frame/ 15 mins for 12 hrs. Scale bars: 50 µm.

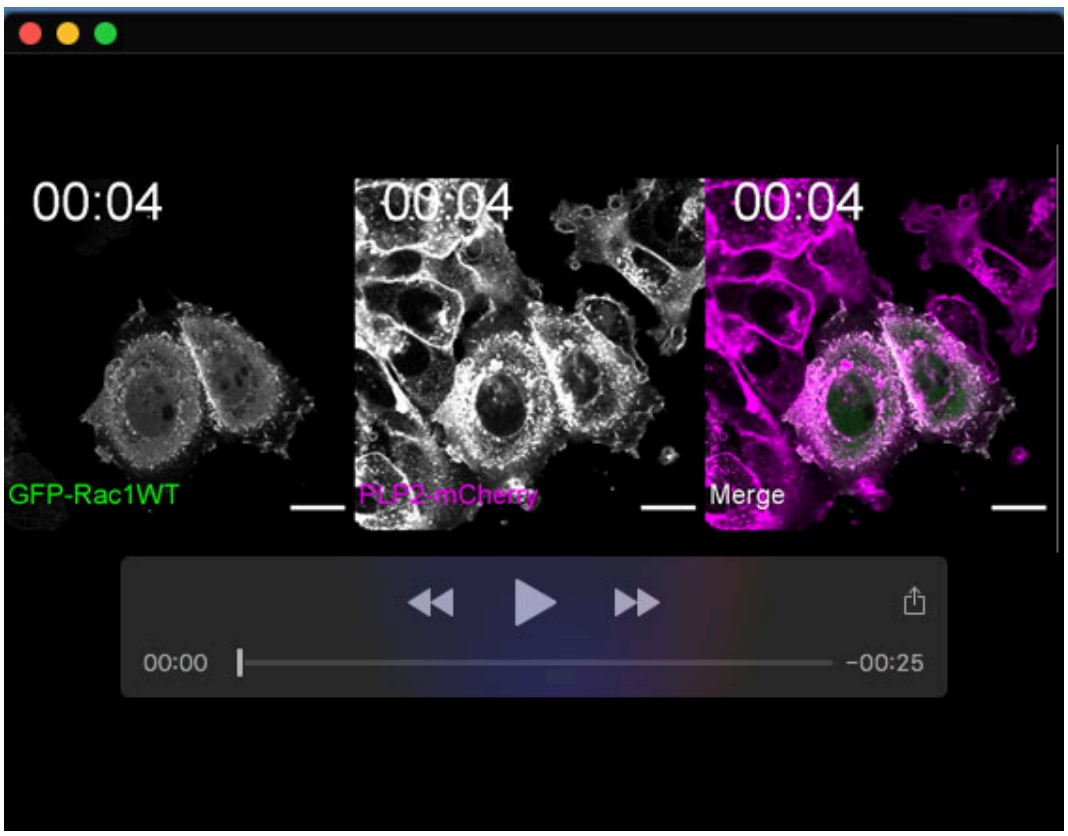

Movie 11. Colocalization dynamics of Rac1-GFPWT and PLP2-mCherry during migration at 4 hrs post wound creation. 1 frame/ 4 mins for 36 mins. Scale bars: 15 µm.

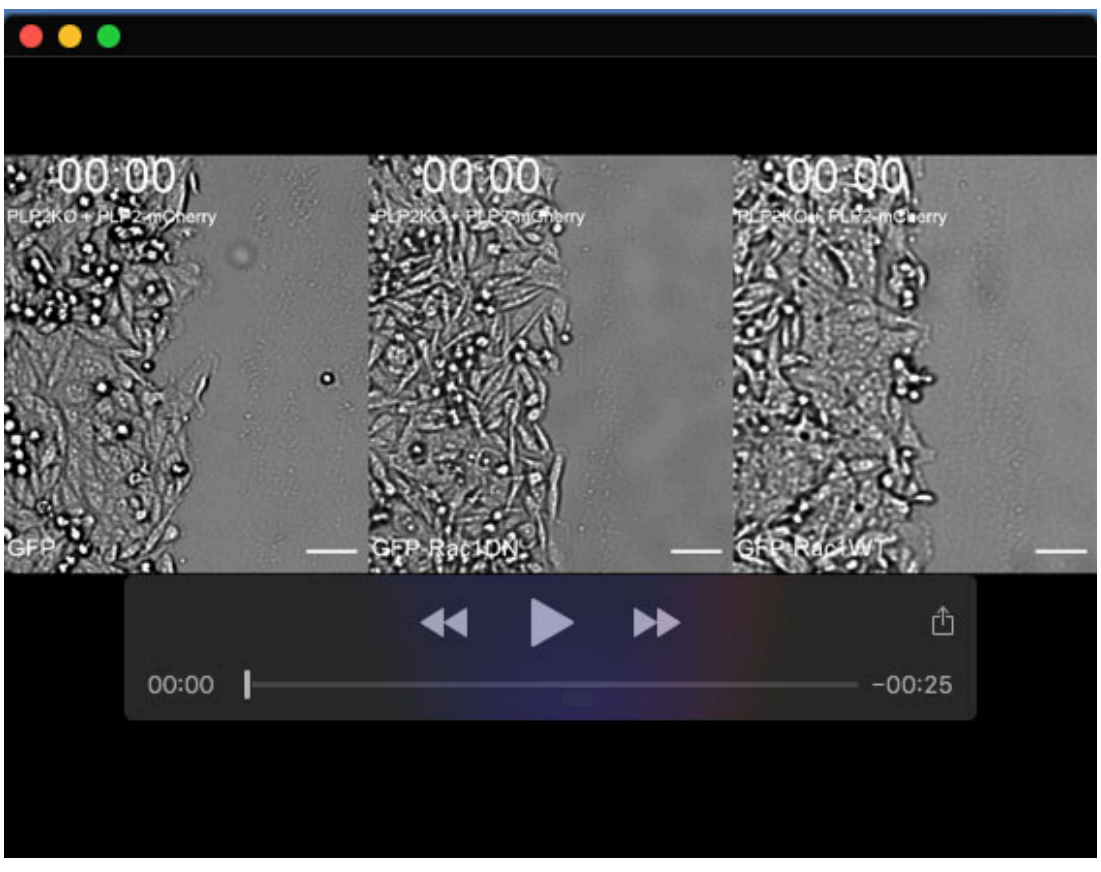

Movie 12. PLP2 mediated collective cell migration involves Rac1 activation. Phase-contrast images of migrating PLP2KO cells co-expressing PLP2-mCherry and GFP (left)/ GFP-Rac1DN (middle)/ GFP-Rac1WT (right) respectively. 1 frame/ 15 mins for 12 hrs. Scale bars: 50 µm.